

OUTFLOW POSITIVITY LIMITING FOR HYPERBOLIC CONSERVATION LAWS. PART I: FRAMEWORK AND RECIPE

EVAN ALEXANDER JOHNSON* AND JAMES A. ROSSMANITH†

Abstract. To support physically faithful simulation, numerical methods for hyperbolic conservation laws are needed that efficiently mimic the constraints satisfied by exact solutions, including material conservation and positivity, while also maintaining high-order accuracy and numerical stability. Finite volume methods such as discontinuous Galerkin (DG) and weighted essentially non-oscillatory (WENO) schemes allow efficient high-order accuracy while maintaining conservation. Positivity limiters developed by Zhang and Shu and summarized in [*Proc. R. Soc. A* **467**, 2752 (2011)] ensure a minimum time step for which positivity of cell average quantities is maintained without sacrificing conservation or formal accuracy; this is achieved by linearly damping the deviation from the cell average just enough to enforce a cell positivity condition that requires positivity at boundary nodes and strategically chosen interior points.

We assume that the set of positive states is convex; it follows that positivity is equivalent to scalar positivity of a collection of affine functionals. Based on this observation, we generalize the technique of Zhang and Shu to a framework that we call outflow positivity limiting: First, enforce positivity at boundary nodes. If wave speed desingularization is needed, cap wave speeds at physically justified maxima by using remapped states to calculate fluxes. Second, apply linear damping again to cap the boundary average of all positivity functionals at the maximum possible (relative to the cell average) for a scalar-valued representation positive in each mesh cell. This be done by enforcing positivity of the *retentional*, an affine combination of the cell average and the boundary average, in the same way that Zhang and Shu would enforce positivity at a single point (and with similar computational expense). Third, limit the time step so that cell outflow is less than the initial cell content.

We show that enforcing positivity at the interior points in Zhang and Shu’s method is actually a means of capping boundary averages at the maximum possible for a positive solution. Capping boundary averages allows computational interior points to be chosen without sacrificing the guaranteed positivity-preserving time step so as to optimize stabilization benefits relative to computational expense, e.g. by choosing points that coincide with nodal points of a DG scheme.

Key words. Nonlinear Hyperbolic Conservation Laws, Finite Volume Methods, Discontinuous Galerkin Finite Element Method, Positivity Limiters, Explicit Time-Stepping

AMS subject classifications. 35L02, 65M60, 65M20

1. Introduction. Consider a variable-coefficient hyperbolic scalar partial differential equation (PDE) of the form

$$\partial_t u(t, \mathbf{x}) + \nabla \cdot \mathbf{f}(t, \mathbf{x}, u) = 0 \quad \text{for } \mathbf{x} \in \Omega, t \in \mathbb{R}_{\geq 0}, \quad (1.1)$$

where $\Omega \subset \mathbb{R}^D$ is the physical domain, t is the time coordinate, $\nabla \cdot$ represents the divergence with respect to \mathbf{x} , $u : \mathbb{R}_{\geq 0} \times \mathbb{R}^D \rightarrow \mathbb{R}$ is a conserved scalar quantity, and the flux function $\mathbf{f} : \mathbb{R}_{\geq 0} \times \mathbb{R}^D \times \mathbb{R} \rightarrow \mathbb{R}^D$ is assumed differentiable. Assume that solutions of (1.1) are positivity-preserving: that is, if $u(0, \mathbf{x}) \geq 0$, then $u(t, \mathbf{x}) \geq 0$ for all $t > 0$. The context of this work will mostly be restricted to a single mesh cell in the interior of the domain, so we do not concern ourselves with boundary conditions for the PDE.

A numerical method for equation (1.1) evolves a numerical solution U that approximates u and is represented by a finite number of degrees of freedom; we say that the method is *accurate* if the error $\|U - u\|_\infty$ vanishes as the degrees of freedom are increased in an appropriate way.

*KU Leuven, Department of Mathematics, Celestijnenlaan 200B box 2400, BE-3001 Heverlee, Belgium (e.alec.johnson@gmail.com).

†Iowa State University, Department of Mathematics, 396 Carver Hall, Ames, IA 50011, USA (rossmani@iastate.edu)

Assumed properties and requirements

We assume a hyperbolic conservation law of the form

$$\partial_t \underline{u}(t, \mathbf{x}) + \nabla \cdot \underline{\mathbf{f}}(t, \mathbf{x}, \underline{u}) = 0, \quad (1.2)$$

where hyperbolicity means that the flux Jacobian matrix $(i, j) \mapsto \hat{\mathbf{n}} \cdot \frac{\partial \underline{\mathbf{f}}_i}{\partial u_j}$ is diagonalizable with real eigenvalues and a full set of eigenvectors for any unit direction vector $\hat{\mathbf{n}} \in \mathbb{R}^D$, where $\|\hat{\mathbf{n}}\| = 1$. Each eigenvalue is a wave speed. Valid physical solutions violate the differential form (1.2) at shock discontinuities but still satisfy the integral form of conservation law (1.2),

$$d_t \int_K \underline{u} + \oint_{\partial K} \hat{\mathbf{n}} \cdot \underline{\mathbf{f}} = 0, \quad (1.3)$$

for arbitrary K . We assume that there is a convex set \mathcal{P} (satisfying $s\mathcal{P} + (1-s)\mathcal{P} \subset \mathcal{P} \forall s \in [0, 1]$) of *positive states* such that \mathcal{P} is an *invariant domain*: if the initial data $\underline{u}(0, \mathbf{x})$ is in \mathcal{P} then the physical solution remains in \mathcal{P} for all time: $\underline{u}(t, \mathbf{x}) \in \mathcal{P} \forall t \geq 0$. Furthermore, we assume that $\underline{\mathbf{f}} \rightarrow 0$ on the boundary of \mathcal{P} . Positivity limiters yield a numerical method that is high-order accurate for smooth solutions and satisfies a discrete local conservation law like (1.3) and a discrete local positivity condition $\int_K \underline{u} \in \mathcal{P}$, where K is restricted to a union of mesh cells.

Fig. 1.1: Assumptions and requirements of positivity limiting (Section 1).

Accuracy is not the only goal of a numerical method, however. One also seeks *physicality* of numerical solutions. If a physical condition is maintained by the solution, then it is desirable for a numerical method to mimic this by maintaining a discrete version of this condition. Such methods are referred to as *mimetic* or *conforming*.

For example, in a problem where material is conserved, the solution u is restricted for all time to a manifold of solutions that have the same total amount of material. A numerical method that fails to satisfy a discrete material conservation law can over time drift from this manifold, resulting in unphysical behavior. Although one can correct for this by a global adjustment to the solution, such an approach still can yield locally incorrect physics. Specifically, solutions that fail to satisfy a discrete *local* conservation law result in simulated shocks that travel at incorrect speeds (see e.g. pages 237–239 of LeVeque [8]).

Similarly, in a problem where the solution should remain positive, a numerical solution that fails to maintain a discrete positivity condition could drift from the set of positive solutions, resulting in an unphysical or even unstable solution. Again, one could globally damp the deviation from the global average. But to ensure local physicality and stability, positivity preservation should be enforced in a *local* manner.

Finite volume methods are called *conservative* because they are designed to mimic the conservation property of conservation laws. Positivity-preserving methods are designed to mimic the positivity-preserving property. The challenge of positivity limiting is to design finite volume methods that are conservative, positivity-preserving, high-order accurate, and numerically stable.

Generalizing to hyperbolic systems, the fundamental assumptions and require-

ments for positivity limiting are summarized in Figure 1.1.

1.1. Historical overview. Consider a 1D conservation law

$$\partial_t u(t, x) + \partial_x f(u) = 0$$

which maintains the condition $u \geq 0$.

A finite volume method partitions the domain into intervals called mesh cells. On a mesh cell of width Δx centered at $x = x_i$ we denote the numerical cell average at time t^n by \bar{U}_i^n :

$$\bar{U}_i^n := \frac{1}{\Delta x} \int_{x_i - \frac{\Delta x}{2}}^{x_i + \frac{\Delta x}{2}} U(t^n, x) dx. \quad (1.4)$$

An Euler step for a method-of-lines finite volume method (e.g., DG or WENO) updates the cell average as follows:

$$\bar{U}_i^{n+1} = \bar{U}_i^n - \frac{\Delta t}{\Delta x} [h(U_{i+1/2}^-, U_{i+1/2}^+) - h(U_{i-1/2}^-, U_{i-1/2}^+)] \quad (1.5)$$

where $U_{i-1/2}^-$ and $U_{i-1/2}^+$ are approximate solution values on the left and right of cell interface $x_{i-1/2}$, respectively, and the numerical flux $h(U^-, U^+)$ is consistent with physical flux: $h(u, u) = f(u)$.

In our abstract setting, what we know about \mathbf{f} is that it is defined so that physical solutions maintain positivity. Therefore, to maintain positivity in the numerical scheme, the numerical flux is defined in terms of the solution to a physical problem. This insight lead to the first general positivity-preserving scheme: the **Godunov scheme**[5], which iterates the following:

1. In each mesh cell replace the solution with its average value.
2. Physically evolve the solution for a time step Δt .

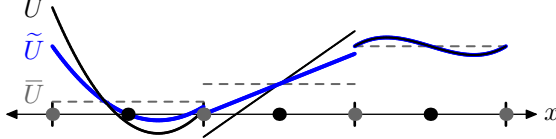
If Δt is sufficiently short, then the flux at each interface is given by the solution to a *Riemann problem*; this is guaranteed if $\Delta t \lambda < \Delta x$, where λ is the sum of left-going and right-going signal speeds propagating from each interface in the physical solution; see Figure 2.1. In this case, the Godunov scheme can be implemented by equation (1.5) if the numerical flux $h(U^-, U^+)$ is chosen to be the interface flux of the Riemann problem with initial states (U^-, U^+) and the solution is assumed to be constant in each cell. A simpler choice of h which maintains positivity in update (1.5) is the HLL numerical flux function [6]. The HLL flux is defined to account for the transfer of material implied by the solution to the Riemann problem modified by averaging in an interval that contains the signals emanating from the interface. To show that HLL preserves positivity, Perthame and Shu [11] used a modified Godunov scheme: before averaging in each mesh cell, the physically evolved solution is first averaged in a set of nonoverlapping intervals each of which contains the signals emanating from one of the interfaces. The Godunov scheme is unfortunately only first-order accurate in space.

To achieve high-order accuracy in space, the numerical flux function h used in update (1.5) needs to accurately approximate the physical flux f . This will be the case if h is consistent with the physical flux and if U^- and U^+ are both high-order accurate approximations to the exact solution at the interface. Therefore, we assume in each cell a representation of the solution of the form

$$U_i^n(x) := \bar{U}_i^n + dU_i^n, \quad (1.6)$$

where \bar{U}_i^n is the cell average and dU_i^n is a high-order correction that is a polynomial of degree at most k . The DG method evolves such a representation, and WENO

Conservative local accuracy-preserving positivity limiting by linear damping of the deviation from the cell average



The positivity limiting framework introduced by Liu and Osher [10] achieves high-order accuracy while maintaining positivity of the cell average \bar{U} in each mesh cell. Prior to each time step the deviation from the cell average is linearly damped until a cell positivity condition is satisfied; a time step is then calculated that preserves positivity of the cell average. Zhang and Shu [16] reduce the cell positivity condition from positivity at every point in the mesh cell (i.e. for an infinite collection of point evaluation functionals) to positivity at a *finite* collection of *positivity points*. The limited solution is $\tilde{U} := \bar{U} + \theta(U - \bar{U})$, where $\theta \in [0, 1]$ is just small enough so that \tilde{U} is positive at each (black) interior point and at each (gray) boundary node.

Fig. 1.2: Positivity limiting illustrated for 1D mesh cells with cubic polynomials.

reconstructs such a representation with each time step. The flux function h remains unchanged (i.e. is defined using the Riemann problem with states U^- and U^+ .)

High-order accurate positivity limiters were developed in the seminal works of Zhang [15] and Zhang and Shu [16]. An in-depth review of the history of this method can be found in the excellent review article [18]. As depicted in Figure 1.2, in each mesh cell they linearly damp the high-order corrections just enough to enforce positivity at a set of strategically chosen positivity points. For concreteness, we describe their method in detail for the 1D scalar case. Let $K = [x_i - \Delta x/2, x_i + \Delta x/2]$ denote a mesh cell, and let $\{s_j\}_{j=0}^{\tilde{n}}$ denote the points of the Gauss-Lobatto quadrature rule that has just enough points to exactly integrate polynomials of degree at most k .

As depicted in figure 1.2, to limit U_i^n , linearly damp dU_i^n just enough to ensure that the solution is positive at each quadrature point. In formulas:

$$U_{\min} := \min_j U_i^n(s_j), \quad \theta := \min \left\{ 1, \frac{\bar{U}_i^n}{\bar{U}_i^n - U_{\min}} \right\}, \quad \tilde{U}_i^n(x) := \bar{U}_i^n + \theta dU_i^n. \quad (1.7)$$

We note that $\theta \in [0, 1]$, and in particular, if $U_{\min} \geq 0$, then $\theta = 1$. Finally, the cell averages are updated by using the damped solution in (1.5):

$$\bar{U}_i^{n+1} = \bar{U}_i^n - \frac{\Delta t}{\Delta x} [h(\tilde{U}_{i+1/2}^-, \tilde{U}_{i+1/2}^+) - h(\tilde{U}_{i-1/2}^-, \tilde{U}_{i-1/2}^+)], \quad (1.8)$$

where $\tilde{U}_{i-1/2}^\pm$ are the edge values computed from the limited solution (1.7). We will see that this algorithm maintains accuracy and guarantees the same positivity-preserving time step that is guaranteed if positivity is enforced everywhere in the mesh cell.

Zhang and Shu have extended their positivity limiters to shallow water and gas dynamics [17], as well as to higher-dimensional problems on both Cartesian and unstructured grids [17, 20].

As leveraged in [16], a framework for positivity limiting can also be used to implement a maximum-principle-satisfying scheme. Suppose that the exact (entropy)

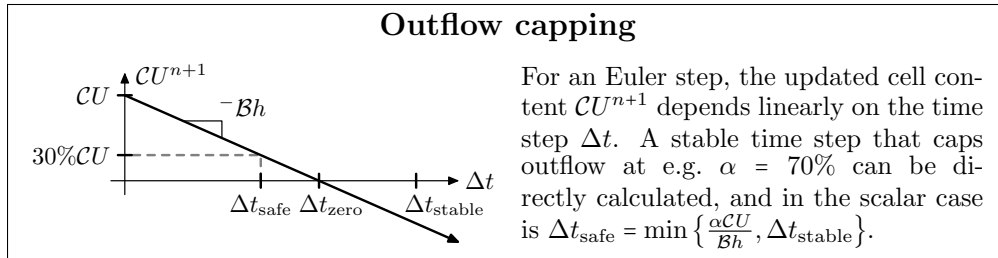


Fig. 1.3: *Outflow capping in the scalar case.*

solution $u(t, x)$ remains bounded in the interval $[U_{\min}, U_{\max}]$. By negation and translation of state space, one can use scalar positivity limiting to enforce that the affine functionals $\bar{U}_i^n - U_{\min}$ and $U_{\max} - \bar{U}_i^n$ are both positive.

1.2. Outflow positivity limiting framework. The main contribution of this work is an analysis and generalization of Zhang and Shu’s positivity limiter based on limiting the potential and actual outflow from each cell. This yields a multi-stage framework we call *outflow positivity limiting*.

1. The first stage is **point-wise positivity limiting**, which consists of enforcing positivity at a set of *positivity points* consisting of *boundary nodes* and *interior points*. Enforcing positivity at boundary nodes ensures that numerical fluxes are defined with positive values. For shallow water and gas dynamics, when positivity of the depth or density is enforced at a boundary node, it is important to calculate fluxes with remapped states in order to desingularize wave speeds. Enforcing positivity at interior points may improve stability.
2. The second stage is **boundary average limiting**. Like Zhang and Shu, we maintain positivity of the cell average by after each time step linearly damping the deviation from the cell average just enough so that a cell positivity condition is satisfied. The essential difference is that our cell positivity condition directly caps the boundary average rather than requiring positivity at points in the cell interior. Specifically, the optimal version of our cell positivity condition requires the boundary average to be no greater than the maximum boundary average possible if the solution were everywhere positive and had the same cell average. Enforcing positivity at the optimal interior points of Zhang and Shu is a means of boundary average limiting.
3. The third stage is **outflow capping**. Rather than restricting the time step to the guaranteed positivity-preserving time step (and assuming that the estimated upper bound on wave speeds is legitimate), we directly calculate a maximal stable time step that caps cell outflow at e.g. 70%. The updated cell average varies linearly with the length of an Euler time step, and therefore outflow capping can be performed with the same limiting procedure that Zhang and Shu use to enforce positivity at a positivity point. See Figure 1.3.

1.3. Benefits of the outflow positivity limiting framework. This framework offers simplicity, insight, flexibility, and computational efficiency. Our framework is implied by a set of natural requirements, e.g. to maintain positivity of the cell average and to guarantee a stable, positivity-preserving time step. We thereby decouple requirements and arrive at a framework that is intrinsic to the requirements and ar-

guably optimal. Outflow capping ensures that knowledge of the fastest wave speed is not needed to compute the positivity-preserving time step. A minimum positivity-preserving time step is guaranteed by positivity of the retentional, which is defined in terms of the data that actually determines the evolution of the cell average (i.e. boundary node data and the initial cell average), and has a physical meaning (cell content minus maximum possible loss). The proof that positivity is maintained is thus intuitively obvious and works for spatially varying flux functions and for arbitrary cell geometry and representation space.

Boundary average limiting can be used to guarantee a positivity-preserving time step even if the data used at the boundary nodes is not interpolated by a polynomial. This is relevant in the gas-dynamics case, where it becomes necessary to modify states at boundary nodes before evaluating fluxes, e.g. to desingularize fluid velocity when enforcing positivity of the density or to enforce realizability or hyperbolicity in higher-moment gas-dynamic models.

Capping the boundary average is enforced via positivity of a single linear functional, the retentional, and is therefore no more expensive than enforcing positivity at a single point. For stabilization purposes, one may additionally enforce positivity at interior points, but the choice of these points can be optimized for requirements of efficiency, simplicity, or stability; if positivity points are instead optimized for maximizing the guaranteed positivity-preserving time step, then enforcing positivity at these points enforces the optimal cap on the boundary average (as illustrated in Figure 1.4.) While we show that such optimal positivity points always exist (see Figure 5.1), precisely isolating them can be non-trivial (in general requiring the solution of linear programming problems on a convex domain), and in the case of nodal DG it is inefficient to check positivity at these non-nodal points if they are relatively numerous. In contrast, outflow positivity limiting merely requires an estimate of the maximum boundary crowding \bar{M}^* realizable by a positive solution. Note that precisely isolating \bar{M}^* also requires solving linear programming problems on a convex domain.

1.4. Parts. This work is conceived of as the first in a three-part series. This first part is analytical rather than computational and avoids making claims dependent on computational experiment; rather, we lay out a general framework that incorporates previous work and that will guide subsequent computational investigation. The second part will give a detailed justification of the analytical results. The third part is planned to consider issues that require computational simulation. In particular, the stability consequences of enforcing positivity at Zhang and Shu’s points, at all nodal points, or only at boundary nodes, will be a natural follow-up study, and results will likely be dependent on the details of the choice of oscillation-suppressing limiters. Since our framework generalizes that of Zhang and Shu, it has in a sense already been computationally tested by their work [14, 15, 16, 17, 18, 19, 20].

1.5. Section summary. The outflow positivity limiting framework is developed in subsequent sections of this paper. In Section 2 we describe how DG (or WENO) updates the cell average. In Section 3 we show in the context of scalar conservation laws that enforcing positivity of the retentional guarantees that the cell average remains positive for a time step inversely proportional to the boundary crowding cap \bar{M} chosen in the definition of the retentional. In Section 4 we show that the same statement holds for hyperbolic systems of conservation laws. In Section 5 we develop a theory of admissible (accuracy-preserving) and optimal cell positivity conditions that shows that, as long as the boundary crowding cap is admissible (i.e. no less than an optimal \bar{M}^*), then enforcing positivity of the retentional by linearly damping the

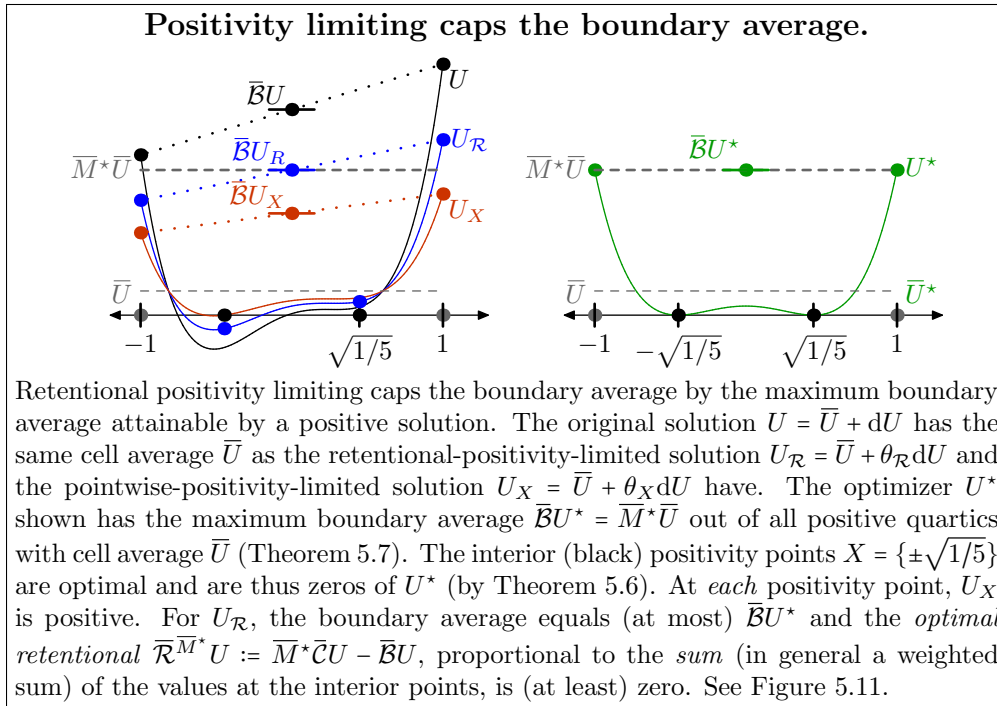


Fig. 1.4: Retentional positivity limiting for a one-dimensional mesh cell with a quartic polynomial basis ($\bar{M}^* = 6$), compared with pointwise positivity limiting.

deviation from the cell average preserves the order of accuracy and can be accomplished by enforcing positivity at strategically chosen interior points. In Section 6 we apply this theory of cell positivity conditions to compute optimal or near-optimal boundary crowding caps and optimal interior points for typical cell geometries and polynomial orders. In Section 7 we discuss practical implementation issues regarding efficiency, robustness, and generalization, with specific reference to shallow water and gas dynamics. These issues include efficient and correct positivity checks, wave speed desingularization, stability benefits of interior positivity points, stable optimal time stepping, multistage and local time stepping, and application to isoparametric mesh cells. In Section 8 we summarize the key results of this work. Boxed figures present a largely self-contained summary of the work.

2. High-order discontinuous Galerkin schemes. For simplicity, we discuss positivity-preserving limiters with reference to the discontinuous Galerkin (DG) method. This does not entail loss of generality, since a WENO finite volume method can be thought of as a DG method that reconstructs the high-order component of the representation prior to each time step. Standard DG schemes discretize the weak form of hyperbolic conservation law (1.1):

$$\frac{d}{dt} \int_K u \varphi = \int_K \mathbf{f} \cdot \nabla \varphi - \int_{\partial K} \hat{\mathbf{n}} \cdot \mathbf{f} \varphi, \quad (2.1)$$

where K is an open subset of \mathbb{R}^D , ∂K is the boundary of K , $\hat{\mathbf{n}}$ is an outward pointing unit vector that at every point on ∂K is perpendicular to the boundary ∂K , and

The **Riemann problem with states** (U^-, U^+) **and flux function** f is defined to be the problem

$$(PDE) \quad \partial_t u(t, x) + \partial_x f(u) = 0, \quad u(0, x) = \begin{cases} U^- & \text{if } x < 0, \\ U^+ & \text{if } x > 0. \end{cases}$$

Riemann problems (and thus their solutions) are by requirement *self-similar*, i.e. invariant under dilation of space-time: $u(at, ax) = u(t, x)$ for any $a > 0$ and $t \geq 0$. So we can write $u(t, x) =: \tilde{u}(x/t)$ for $t > 0$. In hyperbolic problems information propagates at finite speed. Define the **signals** $s^-(t) \leq 0 \leq s^+(t)$ emanating from the *interface* $x = 0$ so that $\sigma := [s^-, s^+]$ is the smallest interval such that $u(t, \cdot)$ agrees with $u(0, \cdot)$ outside σ . By self-similarity, the *signal speeds* \dot{s}^\pm are independent of t and define the **right-going signal speed** $\dot{s}^+(U^-, U^+)$ and **left-going signal speed** $\dot{s}^-(U^-, U^+)$. The *interface flux* f_0 is defined to be the flux at $x = 0$ needed to account for the amount of material that u accumulates on each side of the interface; it is independent of $t > 0$ and equals $f(\tilde{u}(0))$ unless \tilde{u} happens to be discontinuous at 0; then subtracting $\int_{x^-}^0$ (PDE) from $\int_0^{x^+}$ (PDE), applying the fundamental theorem of calculus, and solving reveals that $2f_0 = f(U^-) + f(U^+) + \text{d}_t[\int_0^{x^+} u(t, \cdot) - \int_{x^-}^0 u(t, \cdot)]$ if $x^- < ts^-$ and $x^+ > ts^+$.

Fig. 2.1: Definition of the Riemann problem used to define numerical flux

$\varphi \in C_0^1$ is a test function.

Assume that Ω is the union of a finite set Ω_h of non-overlapping mesh cells. We assume that the solution, when restricted to any mesh cell $K \in \Omega_h$, belongs to a polynomial space $\mathcal{V} = \mathcal{V}(K)$ and is otherwise unconstrained (e.g. by the requirement of continuity across mesh cell boundaries). Often \mathcal{V} is \mathbb{P}_D^k , the set of polynomials in D variables of degree at most k . More generally, we define $\text{deg}(\mathcal{V}) \geq 0$ to be the largest k such that \mathcal{V} contains \mathbb{P}_D^k . The discontinuous Galerkin method approximates the exact solution to (2.1) with a piecewise polynomial function:

$$U|_K = \sum_{i=0}^{N(k)} U^i \varphi_i \in \mathcal{V}, \quad (2.2)$$

where, on each cell K , $\{\varphi^j\}_{j=0}^{N(k)}$ is a basis for $\mathcal{V}(K)$ and $\{\varphi_j\}_{j=0}^{N(k)}$ is its co-basis. The basis and co-basis are mutually orthonormal in the inner product $\frac{1}{|K|} \int_K \varphi^i \varphi_j = \delta_j^i$, where $|K|$ is the measure of the mesh cell K .

In **nodal DG**, the co-basis consists of a set of point-evaluation functionals that evaluate the solution at the nodes, and the solution is thus represented by nodal values. In **modal DG**, the basis is often chosen to be a sequence of orthonormal polynomials of increasing degree. As a consequence, the basis and co-basis are identical and the coefficients of higher-order basis functions decay: specifically, for a smooth function u , the L^2 -projection coefficients $\int_K u \varphi^j$ decay like $\mathcal{O}(\Delta x^{k'+1})$, where Δx is the mesh cell diameter and k' is largest such that $\mathbb{P}_D^{k'} \subset \text{span}\{\varphi^i : i < j\}$.

The DG method solves a discretization of equation (2.1) in each mesh cell K :

$$\frac{d}{dt} \int_K U \varphi^j = \int_K \mathbf{f}(t, \mathbf{x}, U) \cdot \nabla \varphi^j - \oint_{\partial K} h(U^-, U^+, \hat{\mathbf{n}}) \varphi^j, \quad (2.3)$$

Framework of a method-of-lines finite volume Euler step

Integrating the hyperbolic differential equation

$$\partial_t u(t, \mathbf{x}) + \nabla \cdot \mathbf{f}(t, \mathbf{x}, u) = 0$$

over a mesh cell K gives the integral form

$$\frac{d}{dt} \int_K u + \oint_{\partial K} \hat{\mathbf{n}} \cdot \mathbf{f} = 0.$$

Making the replacements $u \rightarrow U \in \mathcal{V}$, $\oint_{\partial K} \rightarrow \mathcal{B}$, and $\hat{\mathbf{n}} \cdot \mathbf{f} \rightarrow h$, where \mathcal{V} is a finite-dimensional representation space, h is a numerical flux, and \mathcal{B} is a numerical boundary quadrature, gives the ordinary differential equation of a method-of-lines finite volume approximation $d_t \mathcal{C}U = -\mathcal{B}h$, where $\mathcal{C} := \int_K$. An Euler step for this ODE is

$$\mathcal{C}U^{n+1} = \mathcal{C}U - \Delta t \mathcal{B}h.$$

Typically \mathcal{V} when restricted to a mesh cell is a polynomial representation space containing all polynomials of degree at most k , $\int_K^Q h = \sum_{\mathbf{x} \in Q} \omega_{\mathbf{x}} h(\mathbf{x})$ is a numerical quadrature rule with points $Q \subset \partial K$ and weights $\omega_{\mathbf{x}} > 0$, and $h(\mathbf{x})$ is a numerical interface flux for the Riemann problem with frozen flux function $f := u \mapsto \hat{\mathbf{n}} \cdot \mathbf{f}(t, \mathbf{x}, u)$ and states (U^-, U^+) (see Figure 2.1); here $U^-(\mathbf{x})$ is the value of U at \mathbf{x} approached from within K and $U^+(\mathbf{x})$ is the value of U at \mathbf{x} approached from outside K . DG and WENO are two ways of updating the deviation of U from the cell average.

Fig. 2.2: The context of this work as outlined in Section 2.

where $\hat{\mathbf{n}}$ is the outward pointing unit normal to ∂K and where $h(U^-, U^+, \hat{\mathbf{n}})$ denotes a numerical flux function where U^- represents the state at the boundary node approached from inside the cell and U^+ represents the state at the same boundary node approached from outside the cell. See Figure 2.2. In equation (2.3) we have replaced exact integration by quadrature rules; in particular, \int_K^Q denotes a quadrature rule exactly equal to \int_K for polynomials of degree at most $2k - 1$ and $\oint_{\partial K}^Q$ denotes a quadrature rule exactly equal to $\oint_{\partial K}$ for polynomials of degree at most $2k$. If K is a polytope then the boundary quadrature rule can be written as the sum over all faces of a Gaussian quadrature rule on each face.

An important property of the DG scheme is that it conserves the total amount of U from time step to time step; indeed, taking $\varphi = 1 \in \mathcal{V}$, equation (2.3) becomes the conservation law

$$\frac{d}{dt} \int_K U = - \oint_{\partial K}^Q h. \quad (2.4)$$

The entire context of this work is concerned with maintaining positivity in a single arbitrary mesh cell. We therefore adopt a simplified notation that omits explicit reference to the mesh cell K . We define the **cell content** to be the cell integral $\mathcal{C} := U \mapsto \int_K U$ or its scale-invariant version, the cell average $\bar{\mathcal{C}} := U \mapsto \int_K U$. We define the **boundary sum** to be the boundary integral quadrature $\mathcal{B} := U \mapsto \oint_{\partial K}^Q U^-$ or its scale-invariant version, the boundary average quadrature $\bar{\mathcal{B}} := U \mapsto \oint_{\partial K}^Q U^-$. We

use $V := |K|$ to denote the “volume” of the mesh cell and $A := |\partial K|$ to denote the “area” of its boundary. With these conventions, the ODE (2.4) is expressed as

$$\begin{aligned} d_t \mathcal{C}U &= -\mathcal{B}h, & \text{i.e.,} \\ d_t \bar{\mathcal{C}}U &= -\bar{\mathcal{B}}\bar{h}, \end{aligned}$$

where $\bar{h} := \frac{A}{V}h$ is a scale-invariant version of the numerical flux, and an explicit Euler step is expressed as

$$\mathcal{C}U^{n+1} = \mathcal{C}U - \Delta t \mathcal{B}h, \quad \text{i.e.,} \quad (2.5)$$

$$\bar{\mathcal{C}}U^{n+1} = \bar{\mathcal{C}}U - \Delta t \bar{\mathcal{B}}\bar{h}. \quad (2.6)$$

This method-of-lines finite volume framework is summarized in Figure 2.2.

3. Framework for outflow positivity limiting. In this work **positive** means *nonnegative* unless qualified with the adjective *strictly*. A *positive combination* means a linear combination with positive coefficients, and a *positive functional* is defined to be a functional that is positive on positive functions.

A simple algorithm that maintains positivity of the cell average is to repeat the following sequence:

1. Assume that the cell average is positive.
2. If necessary, linearly damp (rescale) the deviation from the cell average just enough so that a cell positivity condition is satisfied. (See Figure 1.2.)
3. Execute an Euler step for a stable time step that is just short enough so as to guarantee that positivity of the cell average is maintained (given that the cell positivity condition is satisfied).

This algorithm was first introduced by Liu and Osher [10] and further developed by Zhang and Shu [16].

Assuming that numerical fluxes are calculated by evaluating the flux at the boundary node states (rather than at remapped states), the cell positivity condition should at least require the solution to be positive at the boundary nodes so that the Riemann problem used to define the numerical flux function is well-defined. To ensure that positivity limiting does not compromise order of accuracy, it will be enough to require that the cell positivity condition be satisfied if the initial data is already everywhere positive (as we will verify in Theorem 5.2).

Given the constraints of this framework, we ask: *What cell positivity condition and time step will guarantee that $f_K U^{n+1} \geq 0$?* If we are not allowed to modify a positive solution, then the maximum time step for which we can hope to guarantee positivity is the maximum such time step if the initial data is positive. We therefore ask: *What is the maximum time step for which it is guaranteed that $f_K U^{n+1} \geq 0$ if $U \geq 0$ in K ?* We can assume that the outflow $\mathcal{F}_{\partial K}^Q h$ is strictly positive, since otherwise the cell average will remain positive for any positive time step. In this case, setting $\mathcal{C}U^{n+1} \geq 0$ in equation (2.5) or (2.6) gives

$$\Delta t^{-1} \geq \Delta t_{\text{zero}}^{-1} := \frac{\mathcal{B}h}{\mathcal{C}U} = \frac{\bar{\mathcal{B}}\bar{h}}{\bar{\mathcal{C}}U} \quad (3.1)$$

That is, the time Δt_{zero} until strict positivity of the cell average is violated is the ratio of the total integral of U in the cell to the net rate of flux out of the boundary. Clearly, to guarantee positivity we need a constraint on the flux out of the boundary.

A constraint that extends naturally to systems is to specify a cap on wave speeds. Abstractly we impose that

$$h \leq \lambda U^-, \quad (3.2)$$

where we call λ the **speed cap**; equivalently, $\bar{h} \leq \bar{\lambda} U^-$, where $\bar{\lambda} := \frac{A}{V} \lambda$ is a scale-invariant version of the speed cap. This condition clearly holds for a scalar problem with a convex flux function (e.g. Burgers' equation) if λ is the wave speed, and in Theorem 3.7 we show that for general systems λ can be defined as a cap on the sum of incoming and outgoing signal speeds at each boundary node.

REMARK 3.1 (*omitting bars*). The form of the scale-invariant equations is identical to the form of the non-invariant equations, so we can choose whether to omit or retain bars when discussing general properties.

3.1. Boundary crowding caps and the retentional. Equations (3.1) and (3.2) imply that positivity is maintained if

$$\Delta t^{-1} \geq \lambda \widehat{\mathcal{B}}U = \bar{\lambda} \widehat{\mathcal{B}}U, \quad (3.3)$$

where we call $\widehat{\mathcal{B}}U := \frac{\mathcal{B}U}{\mathcal{C}U}$ or its scale-invariant version $\widehat{\mathcal{B}}U := \frac{\bar{\mathcal{B}}U}{\mathcal{C}U}$ the **boundary crowding**. Therefore, we can guarantee a minimum positivity-preserving time step by enforcing bounds on λ and $\widehat{\mathcal{B}}U$. To maintain order of accuracy, these bounds need to be physically justified. Enforcing a cap on λ is briefly considered in Section 7.2. The focus of this paper is on enforcing a justified cap on $\widehat{\mathcal{B}}U$.

Given that $\bar{M} \geq \widehat{\mathcal{B}}U$, equation (3.3) says that positivity is maintained if

$$\Delta t^{-1} \geq \Delta t_{\text{pos}}^{-1} := \bar{\lambda} \bar{M}. \quad (3.4)$$

To determine a justified \bar{M} , we use that physical solutions satisfy positivity:

DEFINITION 3.2 (\bar{M}^*). We define the **positive solutions** to be the set $\mathcal{V}_K^+ := \{U \in \mathcal{V} : U \geq 0 \text{ in } K \text{ and } \mathcal{C}U > 0\}$ of representations positive and somewhere nonzero in the mesh cell, and we define the **optimal boundary crowding cap** (or **optimal interior weight**) \bar{M}^* to be the maximum boundary crowding over all positive solutions:

$$\bar{M}_K^*(\mathcal{V}) := \sup_{U \in \mathcal{V}_K^+} \widehat{\mathcal{B}}(U). \quad (3.5)$$

We can enforce that $\bar{M} \geq \widehat{\mathcal{B}}U$ in exactly the same way that positivity is enforced at positivity points if we define this condition in terms of positivity of a linear functional:

DEFINITION 3.3 (retentional). Enforcing a cap \bar{M} on $\widehat{\mathcal{B}}U = \frac{\bar{\mathcal{B}}U}{\mathcal{C}U}$ is equivalent to enforcing positivity of the **retentional**¹ $\bar{\mathcal{R}}^{\bar{M}}U := \bar{M}\mathcal{C}U - \bar{\mathcal{B}}U$, or one of its rescaled versions such as $\bar{\mathcal{R}}_{\bar{W}} := \bar{\mathcal{C}}U - \bar{W}\bar{\mathcal{B}}U$, where $\bar{W} := \bar{M}^{-1}$. We call \bar{M} the **interior weight** (or **boundary crowding cap**) and we call \bar{W} the **boundary weight** (or **positivity CFL cap** — see Theorem 3.12).

¹ An abbreviated form of *retention functional*, in the admittedly hokey mathematical tradition of using “adjectivals” as substantives and thus nouns.

CONVENTION 3.4 ($\bar{W} = \bar{M}^{-1}$). Throughout this paper, any symbol involving the letter “W” represents the reciprocal of the corresponding symbol obtained by replacing “W” with “M”.

DEFINITION 3.5 (admissible weights). If $\bar{M} \geq \bar{M}^*$, then we say that \bar{M} and \bar{W} are **admissible** weights, because in this case positivity of U implies positivity of $\bar{\mathcal{R}}^{\bar{M}}$, which means that enforcing positivity of $\bar{\mathcal{R}}^{\bar{M}}$ respects accuracy.

Formally, we have the following two theorems, which comprise the essence of the paper.

3.2. First fundamental theorem of outflow rate limiting.

The first essential theorem of outflow rate limiting is displayed in Figure 3.1. It asserts that at each boundary node the numerical outgoing flux rate h is bounded by the product of the interior value U^- at the node and a speed cap λ ; it assumes that boundary node states are positive and that h preserves positivity for a one-cell problem with states $(0, U^-, U^+)$ and cell width $\Delta x = \lambda$ for any $\Delta t \leq 1$.

REMARK 3.8. Multiplying by cell area over cell volume, $\bar{h}(U^-, U^+) \leq \bar{\lambda}U^-$.

REMARK 3.9. Examples of such a positivity-preserving flux function h are the numerical flux defined by the exact Riemann solver or the Harten-Lax-van Leer (HLL) [6] or local Lax-Friedrichs (LLF) [13] approximate Riemann solvers used with numerical signal speeds that are truly upper bounds for physical signal speeds. See Figure 3.1. LLF is the special case of HLL where the left-going and right-going numerical signal speeds are equal: $\hat{S}^- + \hat{S}^+ = 0$.

REMARK 3.10. If outflow capping is used, then it is not necessary to compute the speed cap λ ; it is sufficient to know that such a finite cap exists.

REMARK 3.11. The proof assumes that Riemann problems are well-defined for vacuum states and involve finite wave speeds. Riemann problems involving vacuum states were considered for gas dynamics in [9]. For the proof it is enough that there exist a sequence of strictly positive states Z_m approaching vacuum such that the lim sup of the signal speeds of the Riemann problems with states (Z_m, U^-) is finite. In systems such as shallow water and gas dynamics for which any state can be connected to the vacuum state without shocks, one can choose states Z_m so that $\hat{s}^+(Z_m, U^-) = |\lambda|_{\max}(U^-)$ for all Z_m ; that is, $\hat{s}^+(0, U^-) = |\lambda|_{\max}(U^-)$.

3.3. Second fundamental theorem of outflow rate limiting.

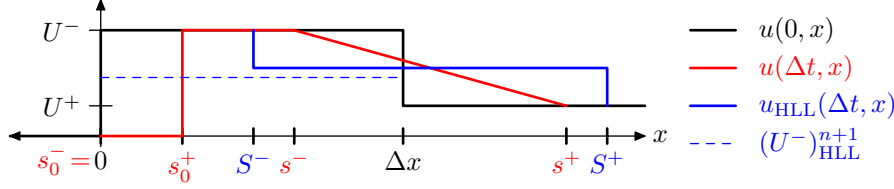
The second essential theorem is displayed in Figure 3.2 and states that if the retentional $\bar{\mathcal{R}}_{\bar{W}} = \bar{C} - \bar{W}\bar{B}$ is positive then an Euler step maintains positivity of the cell average for any time step whose nondimensionalized version $\bar{\lambda}\Delta t$ is no greater than \bar{W} , where λ is a uniform upper bound on the speed cap over all nodes.

The first fundamental theorem can be invoked to satisfy the first hypothesis ($\bar{h} \leq \bar{\lambda}U^-$) of the second fundamental theorem if at each boundary node the numerical flux function is defined using a 1D Riemann problem with frozen flux (see Figure 2.2). The proof of Theorem 3.7 assumes that physical solutions to the two auxiliary Riemann problems are well-defined and maintain positivity. For simplicity, we can impose this assumption rather than assume that the full conservation law (1.2) of Figure 1.1 maintains positivity. But in fact, omitting careful justification, it is an implication of this work that, with appropriate regularity and convergence assumptions, we have:

PROPOSITION 3.13. *The following are equivalent:*

1. *The full system (1.2) maintains positivity.*
2. *Any Riemann problem with positive states and frozen flux function maintains positivity.*

I: $h(U^-, U^+) \leq \lambda U^-$ for a positivity-preserving numerical flux.



DEFINITION 3.6. Define the **one-cell problem with states (Z, U^-, U^+) , cell width Δx , and flux function f** by

$$\partial_t u + \partial_x f(u) = 0, \quad u(0, x) = \begin{cases} Z & \text{if } x < 0, \\ U^- & \text{if } 0 < x < \Delta x, \\ U^+ & \text{if } \Delta x < x; \end{cases} \quad (3.6)$$

it is implied that $Z, U^-, U^+ \geq 0$. Define the **speed cap** to be the sum of the signal speeds entering the cell: $\lambda(Z, U^-, U^+) := s^+(Z, U^-) - s^-(U^-, U^+)$.

THEOREM 3.7 (outflow rate is bounded by speed cap times interior value). *Consider the one-cell problem with states (Z, U^-, U^+) , cell width Δx , and positivity-preserving flux function f . Define the **numerical speed cap** $\lambda := \dot{s}^+(Z, U^-) - \dot{S}^-(U^-, U^+)$, where $\dot{S}^-(U^-, U^+) < \dot{s}^-(U^-, U^+) \leq 0$. Let $h_0(A, B)$ be the interface flux of the Riemann problem with states (A, B) and let $h(A, B)$ be a consistent numerical flux function that preserves positivity for the Euler update*

$$(U^-)^{n+1} = U^- - \frac{\Delta t}{\Delta x} [h(U^-, U^+) - h_0(Z, U^-)] \geq 0 \quad (3.7)$$

if $\lambda \Delta t \leq \Delta x$, i.e., if incoming signals do not cross. Assume that $Z, Z\lambda(Z, Z, U^-)$, and $f(Z)$ all equal or approach 0. Then $h(U^-, U^+) \leq \lambda U^-$.

Proof. Choose $\Delta t = \Delta x / \lambda$. Then (3.7) says that $h(U^-, U^+) \leq \lambda U^- + h_0(Z, U^-)$. But since material cannot flow out of a vacuum, $h_0(Z, U^-) \leq 0$; to verify this rigorously, make the replacements $U^- \rightarrow Z, U^+ \rightarrow U^-$, $h \rightarrow h_0$, and $\lambda \rightarrow \lambda(Z, Z, U^-)$, and use that $h_0(Z, Z) = f(Z)$, which approaches 0. Therefore, $h(U^-, U^+) \leq \lambda U^-$. \square

To see how to define λ and h so that the Euler update (3.7) maintains positivity, for $0 \leq t \leq \Delta t$, let $s_0^-(t) \leq 0 \leq s_0^+(t)$ be the signals emanating from $x = 0$ and let $s^-(t) \leq \Delta x \leq s^+(t)$ be the signals emanating from $x = \Delta x$ (see Figure 2.1). For the HLL flux, the *numerical signal speeds* \dot{S}^- and S^+ are required to satisfy $\dot{S}^- \leq \dot{s}^- \leq 0 \leq \dot{s}^+ \leq \dot{S}^+$. Assume that λ is an upper bound on the sum of the signal speeds \dot{s}_0^+ and $-\dot{S}^-$. Since $\Delta x = \lambda \Delta t$, the signals s_0^+ and $S^\pm(t) := \Delta x + t\dot{S}^\pm$ do not cross (i.e., $s_0^+(\Delta t) \leq S^-(\Delta t) \leq s^-(\Delta t)$). An exact Riemann solver uses the flux of the exact solution at the Δx interface. The HLL solution $u_{\text{HLL}}(t, x)$ equals $u(t, x)$ except in the interval $\mathcal{S}(t) := [S^-(t), S^+(t)]$, where it equals the average value of u in $\mathcal{S}(t)$, $U^*(U^-, U^+) := \frac{f(U^-) - f(U^+) + \dot{S}^+ U^+ - \dot{S}^- U^-}{\dot{S}^+ - \dot{S}^-}$. The flux needed at $x = \Delta x$ to account for the amount of material that u_{HLL} accumulates on each side of the interface defines the HLL numerical flux $h(U^-, U^+) := \frac{1}{2}(f(U^+) + f(U^-)) + (\dot{S}^+ + \dot{S}^-)U^* - \dot{S}^+ U^+ - \dot{S}^- U^-$ (an instance of the formula at the bottom of Figure 2.1).

Fig. 3.1: A signal speed cap and boundary node value bound the outgoing flux rate.

II: A speed cap and positive retentional guarantee a positivity-preserving time step.

THEOREM 3.12. *Suppose that:*

$$\begin{aligned} \bar{h} &\leq \bar{\lambda}U^- \quad (\text{numerical flux is bounded via the speed cap } \bar{\lambda}), \\ \bar{\lambda}\Delta t &\leq \bar{W} \quad (\text{positivity CFL number is bounded by } \bar{W}), \text{ and} \\ \bar{W}\bar{B}U &\leq \bar{C}U \quad (\text{the boundary crowding is capped by } \bar{M} = \bar{W}^{-1}). \end{aligned}$$

Then the updated cell average $\bar{C}U - \Delta t\bar{B}\bar{h}$ is positive.

Proof. $\Delta t\bar{B}\bar{h} \leq \bar{\lambda}\Delta t\bar{B}U \leq \bar{W}\bar{B}U \leq \bar{C}U$. □

Remarks. The proof says that the loss is at most the cell content. The retentional $\bar{\mathcal{R}}_{\bar{W}}U := \bar{C}U - \bar{W}\bar{B}U$ represents the content retained if the maximum possible loss occurs and is positive precisely when the boundary crowding $\bar{B}U/\bar{C}U$ is capped by \bar{M} . Theorem 3.12 is sharp: a smooth example with spatially varying flux function satisfying $\mathbf{f} = \hat{\mathbf{n}}\lambda u$ on ∂K shows that loss can equal cell content. Enforcing positivity of $\bar{\mathcal{R}}^{\bar{M}}$ maintains accuracy for scalar positivity limiting if $\bar{M} \geq \bar{M}^*$.

Fig. 3.2: A speed cap and boundary average cap bound the outgoing flux.

3. The one-cell Euler update (3.7) of Figure 3.1 with an HLL numerical flux function maintains positivity for sufficiently large λ .

Justification. To see that 1 implies 2, assume without loss of generality that the flux function is frozen at $t_0 = 0$ and $\mathbf{x}_0 = 0$ and in the direction $\hat{\mathbf{n}}$. The self-similar solution $u(t, x) = \bar{u}(x/t)$ to the auxiliary Riemann problem with positive states (A, B) can be approximated arbitrarily well by the solution $\tilde{u}(t, \mathbf{x})$ to a multidimensional problem (1.1) with initial data $\tilde{u}_0(\mathbf{x})$ equal to B if $\hat{\mathbf{n}} \cdot \mathbf{x} > 0$, else equal to A . In particular, $\bar{u}(\xi) = \lim_{t \searrow 0} \tilde{u}(t, t\xi\hat{\mathbf{n}})$. We omit a careful justification of this limit, and simply note that f evaluated at $\hat{\mathbf{n}} \cdot \mathbf{x}$ approximates $\hat{\mathbf{n}} \cdot \mathbf{f}$ arbitrarily well for sufficiently small t and \mathbf{x} ; here we rely on the fact that \mathbf{f} is differentiable (hence continuous) and that \tilde{u} by definition depends continuously on \mathbf{f} wherever \tilde{u} is well-defined. Since \tilde{u} satisfies positivity, so do \bar{u} and u .

That 2 implies 3 follows from the definition of HLL in terms of averagings of physical solutions (see Figure 3.1).

That 3 implies 1 follows from the assumption that the positivity-preserving algorithm described in this work converges at least in the first-order case of a representation space that is constant in each cell. We remark that condition 3 gives a practical means of verifying that a physical system maintains positivity. □

3.4. Direct proof for the 1D case. See Figure 3.3.

3.5. Affine-invariant definitions of wave speed and retentional. We have used bars in Sections 2–3 to indicate the scale-invariant formulation. Note that all definitions and statements remain valid if bars are dropped. Alternatively, we can redefine barred quantities using affine-invariant definitions.

Heretofore we have made no distinction between physical and canonical mesh cell coordinates. In general, each physical mesh cell is the image of a *canonical mesh*

Comparison with Zhang and Shu (1D case)

A corollary of the theorems in Figures 3.1 and 3.2 is the 1D case:

COROLLARY 3.14. *The Euler update (1.8) maintains positivity of the cell average if the retentional $\bar{\mathcal{R}}U_i^n := \bar{U}_i^n - \bar{W}\bar{\mathcal{B}}U_i^n$ is positive in each cell and if the time step satisfies $\frac{2\Delta t\lambda}{\Delta x} \leq \bar{W}$, where $\lambda/2$ is an upper bound on signal speeds and $\bar{\mathcal{B}}U_i = \frac{U_{i-1/2}^+ + U_{i+1/2}^-}{2}$ is the boundary average; we assume that the frozen flux function $h_{i+1/2}$ used at any interface is positivity-preserving, in the sense that if it is used at all interfaces then it maintains positivity of cell averages for data constant in each cell if $\lambda \frac{\Delta t}{\Delta x} \leq 1$ (i.e., Δt is short enough that signals from cell interfaces cannot cross in Godunov's method).*

To facilitate comparison with Theorem 2.1 of [17], we offer a direct proof.

Proof. Substituting $\bar{U}_i^n = \bar{\mathcal{R}}U_i + \bar{W}\bar{\mathcal{B}}U_i$ (a boundary-weighted quadrature rule),

$$\begin{aligned} \bar{U}_i^{n+1} &= \bar{U}_i^n - \frac{\Delta t}{\Delta x} \left[h_{i+1/2}(U_{i+1/2}^-, U_{i+1/2}^+) - h_{i-1/2}(U_{i-1/2}^-, U_{i-1/2}^+) \right] \\ &\geq \bar{\mathcal{R}}U_i + \frac{\bar{W}}{2} \left[\begin{aligned} &U_{i+1/2}^- - \frac{2\Delta t}{\bar{W}\Delta x} \left[h_{i+1/2}(U_{i+1/2}^-, U_{i+1/2}^+) - h_{i+1/2}(Z_+, U_{i+1/2}^-) \right] \\ &+ U_{i-1/2}^+ - \frac{2\Delta t}{\bar{W}\Delta x} \left[h_{i-1/2}(U_{i-1/2}^+, Z_-) - h_{i-1/2}(U_{i-1/2}^-, U_{i-1/2}^+) \right] \end{aligned} \right], \end{aligned}$$

which is a positive combination of positive quantities if the Euler steps in brackets satisfy $\frac{2\lambda\Delta t}{\bar{W}\Delta x} \leq 1$; here we take Z_+ and Z_- to be the vacuum state and we use that material cannot flow out of a vacuum: $h_{i+1/2}(Z_+, U_{i+1/2}^-) \leq 0$ and $h_{i-1/2}(U_{i-1/2}^+, Z_-) \geq 0$. Zhang and Shu instead assume a spatially invariant flux function ($h_{i+1/2} = h_{i-1/2}$) and choose $Z_+ = U_{i-1/2}^+$ and $Z_- = U_{i+1/2}^-$. They write the retentional as a weighted sum over interior positivity points (see Theorem 5.6) and choose $\bar{W} = \bar{W}^*$ (see Theorem 6.2). \square

Fig. 3.3: Direct proof for the 1D case.

cell under a coordinate map. In the case of isoparametric mesh cells, the coordinate map is a diffeomorphism, and it is important to work in canonical coordinates. If the coordinate map is affine, however, then we can avoid making a distinction between physical and canonical coordinates if we adopt an *affine-invariant* formulation.

In canonical coordinates, the mesh cell is almost always a cube or simplex and the representation space almost always consists of polynomials. This remains true for isoparametric mesh cells. With an affine-invariant formulation, our results are generally applicable, independent of whether the canonical simplex is defined to be regular or the corner of a box.

In Section 6, we tabulate values or estimates of \bar{M}^* for *regular* canonical polytopes. Thus, when using our tabulated weights to apply the outflow positivity limiting framework, one should take wave speeds to be in terms of their values in the coordinates of a regular canonical mesh cell. A natural way to do this is to use affine invariants.

An affine-invariant formulation of the Euler step (2.5) that agrees with the scale-invariant formulation (2.6) in the case of a regular canonical mesh cell is $\bar{\mathcal{C}}U^{n+1} = \bar{\mathcal{C}}U - \Delta t \bar{\mathcal{B}}^F \bar{h}^F$, where $\bar{\mathcal{B}}^F$ is an affine-invariant version of the boundary average that computes the arithmetic average over all faces of the average on each face; here $\bar{h}_e^F :=$

$\frac{|\mathcal{F}|dA_e}{V}h_e$ is an affine-invariant version of the numerical flux, where dA_e is the area of the face of boundary node e and $|\mathcal{F}|$ is the number of faces of the mesh cell. Similarly, since wave speeds scale like fluxes, if λ_e is a wave speed at boundary node e in the canonical coordinates of mesh cell K , then the quantity $\bar{\lambda}_e^F := \frac{|\mathcal{F}|dA_e}{V}\lambda_e$ is the affine-invariant version that agrees with the scale-invariant version $\bar{\lambda}_e = \frac{A}{V}\lambda_e$ in the case of a canonical regular polytope. In the case of a regular canonical polytope the affine-invariant quantities \bar{h}_e^F , $\bar{\lambda}_e^F$, and $\bar{\mathcal{B}}^F$ agree with their scale invariant equivalents \bar{h}_e , $\bar{\lambda}_e$, and $\bar{\mathcal{B}}$, and the theory of Sections 3–5 goes through.

If one is computing with a non-regular canonical polytope \tilde{K} (e.g. the standard orthogonal simplex defined as the corner of a box) then an affine-invariant definition should be used in the definition of the retentional:

$$\bar{\mathcal{R}}_{\bar{W}}(U) := \bar{\mathcal{C}}U - \bar{W}\bar{\mathcal{B}}^F U. \quad (3.8)$$

If outflow capping is used, then computing wave speeds is not necessary, and use of the boundary face average $\bar{\mathcal{B}}^F$ in the definition (3.8) of the retentional is the only modification needed to implement affine-invariant positivity-limiting.

4. Systems versus scalar case. In the systems case of Figure 1.1, the set of positive states \mathcal{P} is a convex set $\mathcal{P} \subset \mathbb{R}^N$. A corollary of Theorem 3.4 in [12] is that any open or closed convex set is an intersection of half-planes. But any half-plane is the set on which some affine functional A is positive. Therefore, we assume that there exists a set \mathcal{P}^* of affine functionals such that a state $\underline{u} \in \mathbb{R}^N$ is positive if for all $A \in \mathcal{P}^*$ $A(\underline{u}) \geq 0$. We call A a **state positivity functional**. Any such affine functional A decomposes uniquely as $A =: s + \Lambda$, where $s = A(0)$ is a scalar shift and $\Lambda := A - s$ is its **linear part**. Applying A reduces the systems case to the scalar case:

$$\partial_t A(\underline{u}) + \nabla \cdot (\Lambda \mathbf{f}) = 0.$$

After applying A to states and Λ to fluxes, all statements and reasoning of Theorems 3.7 and 3.12 remain valid. For example, the inequality $h \leq \lambda U^-$ becomes the inequality $(\Lambda \underline{h}) \leq \lambda A(\underline{U}^-)$.

Let $\mathcal{R} : \mathcal{V} \rightarrow \mathbb{R}$ be a retentional. Applied component-wise, the retentional defines a state-valued linear map $\tilde{\mathcal{R}} : \mathcal{V} \rightarrow \mathbb{R}^N$, which we identify with \mathcal{R} . Applied point-wise, a state positivity functional $A = s + \Lambda$ defines a map $\tilde{A} = s + \tilde{\Lambda} : \mathcal{V}^N \rightarrow \mathcal{V}$ that we identify with A . Observe that $\mathcal{R}\tilde{\Lambda} = \Lambda\tilde{\mathcal{R}}$. It is desirable that the retentional commute with all state positivity functionals: $\mathcal{R}\tilde{A} = A\tilde{\mathcal{R}}$; then enforcing positivity of $\tilde{\mathcal{R}}$ is the same as enforcing $\mathcal{R}\tilde{A} \geq 0$ for all $A \in \mathcal{P}^*$. This will hold if $\mathcal{R}s = s$, which holds if s is always 0 (that is, if \mathcal{P} is a convex cone) or if the retentional is rescaled so that $\mathcal{R}1 = 1$. Therefore, for any retentional \mathcal{R} we define its **unital retentional** to be $\hat{\mathcal{R}} := \frac{\mathcal{R}}{\mathcal{R}1}$. Then $\hat{\mathcal{R}}1 = 1$. To be concrete: $\hat{\mathcal{R}}^M = \frac{MC - \mathcal{B}}{M - 1}$; we remark that $\hat{\mathcal{R}}$ is an affine combination of state values and therefore is invariant under translation of state space.

For typical systems such as shallow water and gas dynamics, the set of positive states is a convex cone (i.e. invariant under rescaling), so $s = 0$ and $A = \Lambda$ and there is no need to rescale the retentional to its unital version. We remark that by adding the trivial equation $\partial_t u_{\text{extra}} = 0$ to the system, where u_{extra} is a scalar taken to be 1 for physical solutions, defining the set of positive states to be $\{(ru, r) : u \in \mathcal{P}, r \geq 0\}$, and extending each positivity functional $A = s + \Lambda$ to the linear functional $\tilde{\Lambda} := (u, u_{\text{extra}}) \mapsto su_{\text{extra}} + \Lambda u$, the set of positive states can be assumed without loss of generality to be a convex cone.

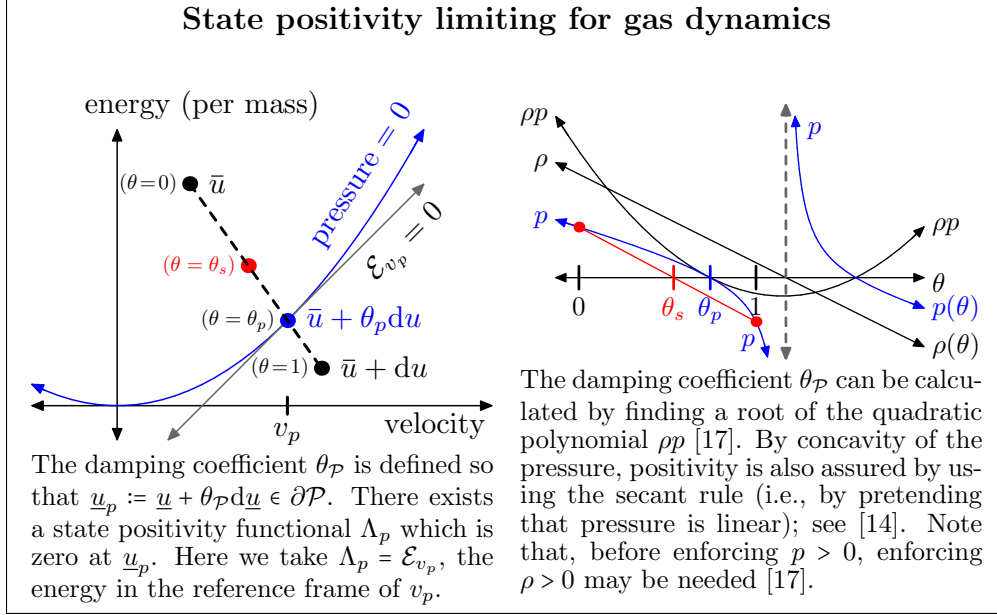


Fig. 4.1: Depiction of positivity limiting of a state value for Euler gas dynamics. Positivity limiting requires determining where a linear path in state space intersects the boundary of positive states.

While we can assume the scalar case without loss of generality when it comes to the *positivity-preserving* results of Section 3, the *accuracy* result of Theorem 5.2 does not go through e.g. to the gas-dynamics case (see Section 4.2).

4.1. State positivity indicators.

Outflow positivity requires the solution to the following problems:

1. To cap outflow, determine the largest value of $\theta \in [0, 1]$ for which $u(\theta) := \bar{u} + \theta du$ satisfies positivity, where $\bar{u} = \mathcal{C}U$ and $du = \Delta t_{\max} \mathcal{B}h$.
2. To cap boundary crowding at \bar{M} , determine the largest value of $\theta \in [0, 1]$ for which $u(\theta) := \bar{u} + \theta du$ satisfies positivity, where $\bar{u} = \bar{\mathcal{R}}\bar{U}$, $du = \bar{\mathcal{R}}dU$, $\bar{\mathcal{R}} := (\bar{\mathcal{R}}^M 1)^{-1} \bar{\mathcal{R}}^M$, and $\bar{\mathcal{R}}^M := \bar{M}\bar{\mathcal{C}} - \bar{\mathcal{B}}$.
3. To enforce positivity at \mathbf{x}_0 , determine the largest value of $\theta \in [0, 1]$ for which $u(\theta) := \bar{u} + \theta du$ satisfies positivity, where $\bar{u} = \bar{U}$ and $du = dU(\mathbf{x}_0)$.

All these problems seek the intersection of a line segment with the boundary of a convex set of states designated positive and require computing a damping coefficient:

DEFINITION 4.1. Let $\bar{\mathcal{P}}$ be a closed convex set of states deemed positive, and let \mathcal{P}^* be a collection of affine functionals such that $\bar{\mathcal{P}} = \{u \in \mathbb{R}^N : (\forall A \in \mathcal{P}^*) Au \geq 0\}$. Let $A \in \mathcal{P}^*$. Let $\bar{u}, u \in \mathbb{R}^N$, where $\bar{u} \in \bar{\mathcal{P}}$. Define $du := u - \bar{u}$. Define $\theta_A(\underline{u}, d\underline{u})$ to be the largest $\theta \in [0, 1]$ such that $A(\bar{\theta}\bar{u} + \theta u) \geq 0$, where we define $\bar{\theta} := 1 - \theta$. Define $\theta_{\mathcal{P}}(\bar{u}, u)$ to be the largest $\theta \in [0, 1]$ such that $\bar{\theta}\bar{u} + \theta u \in \bar{\mathcal{P}}$. Observe that $\theta_A(\bar{u}, u)$ equals 1 if $A(u) \geq 0$ and else equals $\frac{A\bar{u}}{A\bar{u} - Au} = \frac{s + \Lambda\bar{u}}{-\Lambda du}$. Observe that $\theta_{\mathcal{P}}(\underline{u}, d\underline{u}) = \min_{A \in \mathcal{P}^*} \theta_A(\underline{u}, d\underline{u})$.

If \mathcal{P}^* is a finite set, then it can be used directly to calculate $\theta_{\mathcal{P}}$, as illustrated in Figure 1.3 for the case of scalar outflow capping. In the example of Euler gas

dynamics, however, the state is positive if the energy in an arbitrary reference frame (a linear functional of conserved variables) is positive. But such energies comprise an infinite collection \mathcal{P}^* of linear functionals. Instead, one can use the density ρ (a linear functional), and pressure p (a concave nonlinear functional, see section 3.1 of [14]) or ρp (a quadratic functional of conserved variables, see [17]) as a finite set of positivity indicators. See Figure 4.1.

4.2. Accuracy of positivity limiting in the systems case. For the case of scalar conservation laws, accuracy of pointwise positivity limiting via linear damping is established in Section 5 based on Theorem 5.2.

In the case of shallow water, positive states are characterized by positivity of a single linear functional (the depth). Therefore, the proof of accuracy for the scalar case can be invoked to conclude that positivity limiting does not compromise accuracy of the water depth. Assuming that fluid velocities are bounded, this in turn implies that positivity limiting does not compromise accuracy of the solution as a whole.

But in the case of gas dynamics, one must also enforce positivity of the pressure. There exist physical solutions with arbitrarily large and rapid variation in density for which the pressure remains arbitrarily close to zero. Therefore, if positivity is enforced by damping the deviation of the cell average by a scalar value of $\theta \in [0, 1]$, then a given amount of damping needed to enforce positivity of the pressure can entail damping of the density variation that is arbitrarily large in magnitude.

On the other hand, if the pressure of the exact solution is strictly bounded away from zero, then positivity limiting respects accuracy for the simple reason that positivity limiters are not triggered if the mesh is sufficiently fine, if the exact solution is smooth, and if $\bar{M} > 1$. In this case, positivity limiting is really about practical robustness. The study of accuracy and stability for gas-dynamic problems (or sequences of problems) for which the pressure is not bounded away from zero is delicate and is left to future work.

5. Admissible weights and cell positivity functionals. In this section we show that positivity of the retentional $\mathcal{R}^M(U)$ can be enforced without loss of accuracy as long as the interior weight M is greater than or equal to an optimal value M_K^* and that this holds precisely when positivity of $\mathcal{R}^M(U)$ can be enforced by enforcing positivity at appropriately chosen *interior points* in the mesh cell K (see Figure 1.4).

In Section 6 we use this theory (and interior points in particular) to compute (or isolate) the optimal value \bar{M}^* for important mesh cell geometries and representation spaces. As elsewhere, in this section the following context is assumed:

CONTEXT 5.1. *K is a compact mesh cell (in canonical coordinates) and \mathcal{V} is a finite-dimensional polynomial space which contains the set \mathbb{P}_D^k of all polynomials in D variables of degree at most $k \geq 0$. We always assume that $U \in \mathcal{V}$.*

Recall from equation (3.5) that the optimal interior weight $M^* = M_K^*(\mathcal{V})$ is defined as the supremum of the boundary crowding $\widehat{\mathcal{B}}(U) := \frac{\mathcal{B}(U)}{\mathcal{C}(U)}$ over the set \mathcal{V}_K^+ of all nonzero solutions $U \in \mathcal{V}$ positive in the mesh cell K , where $\mathcal{C}(U) := \int_K U$ and $\mathcal{B}(U) := \oint_{\partial K} U$. The retentional $\mathcal{R}_W(U) := \mathcal{C}(U) - W\mathcal{B}(U)$, or $\mathcal{R}^M(U) := M\mathcal{C}(U) - \mathcal{B}(U)$, is positive for all such positive U precisely when $M := W^{-1}$ is admissible, i.e., when $M \geq M^*$.

The following results will be proved in detail in Part II [7]. We summarize these results in Figure 5.1 and illustrate them in Figure 1.4.

THEOREM 5.2 (An admissible weight preserves accuracy). *Let $M \geq M^*$. Then linearly damping the deviation from the cell average just enough to enforce positivity of the retentional $\mathcal{R}^M(U)$ retains order- k local accuracy.*

Proof (sketch). Since physical solutions are positive, damping the variation from the cell average just enough to enforce positivity everywhere in the mesh cell preserves accuracy; a formal proof uses that the maximum $n_{\max} := dU \mapsto \max(dU(K))$ and the magnitude of the minimum $n_{\min} := dU \mapsto \max(-dU(K))$ are (equivalent) asymmetric norms on the finite-dimensional linear space of polynomials $dU \in \mathcal{V}$ whose cell average is zero (see [18]). If M is an admissible weight, then the retentional $\mathcal{R}^M(U)$ is positive if U is positive everywhere in the mesh cell, so enforcing positivity of $\mathcal{R}^M(U)$ also retains accuracy. \square

THEOREM 5.3 (Enforcing positivity of the points of a nodal scheme is sufficient to enforce a positive retentional for some $M < \infty$). *Let X be a set of points capable of representing the solution and for which the cell average can be represented as a strictly positive combination of point values. Then $M_X^* < \infty$, where $M_X^* := \sup \widehat{\mathcal{B}}(\widehat{\mathcal{V}}_X^+)$ and $\widehat{\mathcal{V}}_X^+ := \{U \in \mathcal{V} : \mathcal{C}U = 1 \text{ and } (\forall \mathbf{x} \in X) U(\mathbf{x}) \geq 0\}$.*

Proof (sketch). If U is positive on X then $\mathcal{C}U > 0$, so $\widehat{\mathcal{B}}(U)$ is continuous on $\widehat{\mathcal{V}}_X^+$. Using that n_{\max} and n_{\min} are equivalent asymmetric norms, one can show that $\widehat{\mathcal{V}}_K^+ := \{U \in \mathcal{V}_K^+ : \mathcal{C}U = 1\}$ is bounded and hence compact. Therefore, $\widehat{\mathcal{B}}(\widehat{\mathcal{V}}_X^+)$ has a finite maximum. \square

THEOREM 5.4 (A boundary-weighted quadrature rule gives an upper bound for the optimal weight). *Suppose that the cell content is given by a boundary-weighted quadrature rule, $\mathcal{C}(U) = \mathcal{R}(U) + W\mathcal{B}(U)$, where the boundary weight W is strictly positive and $\mathcal{R}(U)$ represents a quadrature rule $\sum_{\mathbf{x} \in X} w_{\mathbf{x}}U(\mathbf{x})$ for the retentional $\mathcal{R}_W(U)$ with positive weights $w_{\mathbf{x}}$ that is exact for $U \in \mathcal{V}$. Then $M^* \leq M := W^{-1}$.*

REMARK 5.5. Enforcing positivity at the points X enforces positivity of \mathcal{R}_W ; we call X a set of **retentional** (or **interior**) **points** for the weight M .

Proof. Indeed, $\mathcal{R} = \mathcal{C} - W\mathcal{B}$ is positive for all U positive in K , so for any positive U , $W^{-1} \geq \frac{\mathcal{B}(U)}{\mathcal{C}(U)} = \widehat{\mathcal{B}}(U)$, so W^{-1} is an upper bound on M^* . \square

THEOREM 5.6 (An optimal boundary-weighted quadrature rule exists). *An optimal quadrature rule $\mathcal{C}(U) = \sum_x w_x U(\mathbf{x}) + W\mathcal{B}(U)$ exists such that $M^* = W^{-1}$.*

Proof (sketch). If X is a subset of K , then \mathcal{R}^M is positive on $\widehat{\mathcal{V}}_X^+$ if $M \geq M_X^* := \sup \widehat{\mathcal{B}}(\widehat{\mathcal{V}}_X^+)$ and thus (if X is a finite set) is representable as a positive combination of values at a subset $\tilde{X} \subset X$ of points which comprise linearly independent point evaluation functionals; a compactness argument extends this statement from finite X to $X = K$. \square

THEOREM 5.7. *An optimizer $U^* \in \mathcal{V}_K^+$ exists such that $M^* = \widehat{\mathcal{B}}(U^*)$.*

Proof (sketch). By definition, M^* is defined to be the supremum of the boundary crowding $\widehat{\mathcal{B}}(U) := \frac{\mathcal{B}(U)}{\mathcal{C}(U)}$ over all nonzero U positive in the mesh cell K . Thus, any U positive on K gives a lower bound $\widehat{\mathcal{B}}(U)$ on M^* . The question is whether an arg max of $\widehat{\mathcal{B}}$ exists. Since $\widehat{\mathcal{B}}$ is continuous $\widehat{\mathcal{V}}_K^+$ and $\widehat{\mathcal{V}}_K^+$ is compact (see the proof of Theorem 5.2), an arg max U^* of $\widehat{\mathcal{B}}$ exists. \square

Thus, it is possible to determine the optimal weight M^* and a set of optimal retentional points simply by guessing an optimizer and an optimal boundary-weighted quadrature rule and using them to confirm one another. We now identify properties that reduce the set of guesses that we have to consider.

THEOREM 5.8 (Invariance under isometries can be required of retentional points and optimizer candidates).

Proof (sketch). A typical canonical mesh cell has a group of isometries; by averaging over an orbit, for any solution U there exists a \tilde{U} invariant under the action of the group of isometries of the mesh cell with the same values of \mathcal{C} , \mathcal{B} , and $\widehat{\mathcal{B}}$. Similar averaging shows that every boundary-weighted quadrature rule $\mathcal{C}(U) =$

Optimal accuracy-respecting cell positivity functionals

Assume Context 5.1: K is a compact mesh cell, \mathcal{V} is a finite-dimensional polynomial space which contains the set \mathbb{P}_D^k of all polynomials in D variables of degree at most $k \geq 0$, $\bar{\mathcal{C}}U := f_K U$, $\bar{\mathcal{B}}U := f_{\partial K} U$, $\widehat{\mathcal{B}}U := \bar{\mathcal{C}}U/\bar{\mathcal{B}}U$, $\mathcal{V}_K^+ := \{U \in \mathcal{V} : \inf U(K) \geq 0, \bar{\mathcal{C}}U > 0\}$, $\bar{M}^* := \sup \widehat{\mathcal{B}}(\mathcal{V}_K^+)$, and $\bar{\mathcal{R}}^{\bar{M}} := \bar{M}\bar{\mathcal{C}} - \bar{\mathcal{B}}$. Then the following results hold:

COROLLARY 5.11 (existence of an invariant optimizer and of invariant retentional points which isolate the optimal weight). *Linearly damping the deviation from the cell average just enough to enforce positivity of the retentional $\bar{\mathcal{R}}^{\bar{M}}$ retains order- k local accuracy as long as \bar{M} is admissible, i.e., $\bar{M} \geq \bar{M}^*$ (Theorem 5.2). Any solution $U \in \mathcal{V}$ positive in K and any correct boundary-weighted quadrature rule $\bar{\mathcal{C}}(U) = \sum_{\mathbf{x} \in X} \bar{w}_{\mathbf{x}} U(\mathbf{x}) + \bar{W}\bar{\mathcal{B}}(U)$ give a bracket $\widehat{\mathcal{B}}(U) \leq \bar{M}^* \leq \bar{W}^{-1}$ for the optimal weight (Theorem 5.4). Furthermore, an optimizer U^* exists (Theorem 5.7) and an optimal boundary-weighted quadrature rule exists (Theorem 5.6) such that the bracket is an equality: $\widehat{\mathcal{B}}(U^*) = \bar{M}^* = \bar{W}^{-1}$. Enforcing positivity at the set X of **retentional points** enforces positivity of the retentional $\bar{\mathcal{R}}^{\bar{M}}$ (see Remark 5.5). The zero-set of U^* is nonempty if $\bar{M}^* \neq 1$ (Theorem 5.10) and must contain X if X is optimal (by Theorem 5.6). All these statements continue to hold if the optimizer U^* or the quadrature rule (i.e. the retentional points X and the quadrature weights $\bar{w}_{\mathbf{x}}$) is required to be invariant under the action of the isometries of the mesh cell (Theorem 5.8).*

Fig. 5.1: Summary of the results of Section 5.

$\sum_{\mathbf{x} \in X} w_{\mathbf{x}} U(\mathbf{x}) + W\mathcal{B}(U)$ has an invariant version $\mathcal{C}(U) = \sum_{\mathbf{x} \in \tilde{X}} \tilde{w}_{\mathbf{x}} U(\mathbf{x}) + W\mathcal{B}(U)$. \square

LEMMA 5.9 (The boundary crowding of a positive combination of two functions with positive cell average is a convex combination of their boundary crowding values). *Let $U, V \in \mathcal{V}_K^+$. Let $s > 0$ and $t > 0$. Then $\widehat{\mathcal{B}}(sU + tV) = a\widehat{\mathcal{B}}(U) + (1-a)\widehat{\mathcal{B}}(V)$ for some $a \in (0, 1)$.*

Proof. $\widehat{\mathcal{B}}(sU + tV) = \frac{s\bar{\mathcal{B}}U + t\bar{\mathcal{B}}V}{s\bar{\mathcal{C}}U + t\bar{\mathcal{C}}V} = a\widehat{\mathcal{B}}(U) + (1-a)\widehat{\mathcal{B}}(V)$, where $a = \frac{s\bar{\mathcal{C}}U}{s\bar{\mathcal{C}}U + t\bar{\mathcal{C}}V}$. \square

THEOREM 5.10 (A non-constant optimizer has a zero). *An optimizer U^* has a zero in K unless $U = 1$ is an optimizer (in which case $\bar{M}^* = 1$).*

Proof. We have that $\bar{M}^* = \widehat{\mathcal{B}}U^*$. Let $U_{\min} := \min U^*(K)$. Assume that $U_{\min} > 0$. Let $\tilde{U} := U^* - U_{\min}$. Since $\widehat{\mathcal{B}}(U_{\min}) = 1$, by Lemma 5.9, $\widehat{\mathcal{B}}(U^*) = \widehat{\mathcal{B}}(\tilde{U} + U_{\min}) = a\widehat{\mathcal{B}}(\tilde{U}) + (1-a)$, for some $0 < a < 1$. If $\widehat{\mathcal{B}}(\tilde{U}) < 1$ then $\widehat{\mathcal{B}}(U^*) < 1 = \widehat{\mathcal{B}}(U_{\min})$, contradicting the maximality of $\widehat{\mathcal{B}}(U^*)$. If $\widehat{\mathcal{B}}(\tilde{U}) > 1$ then $\widehat{\mathcal{B}}(U^*) < \widehat{\mathcal{B}}(\tilde{U})$, again contradicting the maximality of $\widehat{\mathcal{B}}(U^*)$. Therefore, $\widehat{\mathcal{B}}(U^*) = 1$. But $\widehat{\mathcal{B}}(1) = 1$, so 1 is an optimizer. \square

6. Calculated weights (functional analysis calculations). The previous section developed a general theory of cell positivity functionals. In this section, we use the results of Section 5 summarized in Figure 5.1 to determine retentional points and lower and upper bounds for the optimal weight \bar{M}_K^* for the two standard mesh cell geometries (box and simplex) and for polynomial representation spaces of varying

order. The most important results of this section are summarized in Figure 6.1.

REMARK 6.1 (retaining bars when computing weights). In accordance with Remark 3.1, we dropped bars in the previous section without affecting the validity of the general theorems. In this section, however, we obtain concrete numerical values for the interior weight \bar{M} ; since we want these results to be independent of the scale of the canonical mesh cell, we retain bars in this section.

6.1. Definitions and summary of results. Recall that $\bar{M}_K^*(\mathcal{V})$ denotes the optimal interior weight for mesh cell K with representation space \mathcal{V} . We tabulate values or upper and lower bounds on the optimal interior weights for standard canonical mesh cells: the unit interval $[0, 1]$, the unit square $[0, 1]^2$, the unit cube $[0, 1]^3$, an equilateral triangle Δ^2 , and a regular tetrahedron Δ^3 . Each upper bound \bar{M} constitutes an admissible weight and is calculating using a quadrature rule for the retentional $\bar{\mathcal{R}}^{\bar{M}}$ whose quadrature points can be used as positivity points.

DEFINITION 6.2 (canonical mesh cells). In \mathbb{R}^D , define canonical mesh cells:

$$\begin{aligned} [0, 1]^D &= \text{regular box}, & \bigcirc^D &= \text{sphere}, \\ \Delta^D &= \text{regular simplex}, & \star^D &: \text{“star-regular” polytope.} \end{aligned}$$

We define a **star-regular** polytope to be any star-convex mesh cell that can be centered on the origin to have a constant value of $\hat{\mathbf{n}} \cdot \mathbf{x}$, where $\hat{\mathbf{n}}$ is the outward unit normal and \mathbf{x} is position on the cell boundary. We use \star^D as a generic designation for a star-regular polytope. Regular polytopes are star-regular. Since most often the representation space is \mathbb{P}_D^k , we define

$$\bar{M}_K^k := \bar{M}_K^*(\mathbb{P}_D^k).$$

For practical use, we summarize our calculation of interior weights in Figure 6.1.

6.2. Additional definitions for regular polytopes. To calculate quadrature rules that yield admissible boundary weights for higher-dimensional mesh cells, we try to reduce to a one-dimensional problem using the following symmetry framework.

DEFINITION 6.3 (notation and conventions). Let $\bar{\mathcal{C}} = f_K$ denote the cell average. With star-regular polytopes in mind, assume that the canonical mesh cell is centered on the origin. Define the **radius** r to be $\hat{\mathbf{n}} \cdot \mathbf{x}$, which for a regular polytope is the distance from the origin to the closest point on the boundary of the mesh cell. We will assume unless stated otherwise (and without loss of generality) that the radius of K is 1. Let $\bar{\mathcal{B}}_r$ denote the average over the boundary of the mesh cell rK rescaled to have radius r .

PROPOSITION 6.4 (The cell average is a weighted average of boundary averages over rescaled cells). *Let K be a star-regular polytope in D -dimensional space. Then*

$$\bar{\mathcal{C}} = \frac{\int_0^1 r^{D-1} \bar{\mathcal{B}}_r dr}{\int_0^1 r^{D-1} dr} = D \int_0^1 r^{D-1} \bar{\mathcal{B}}_r dr. \quad (6.1)$$

Furthermore, if the polynomial representation space \mathcal{V} is a subset of \mathbb{P}_D^k then $\bar{\mathcal{B}}_r$ is a polynomial in r of degree at most k .

Proof. Equation (6.1) equates weighted averages and is justified by observing that the thickness of the infinitesimal shell $[r, r + dr] \cdot K$ is dr and its area is proportional to r^{D-1} . Since any polynomial is a sum of homogeneous polynomials, to justify the final statement it is enough to observe that the statement is correct for homogeneous polynomials; indeed, if U is homogeneous of degree k' then so is $\bar{\mathcal{B}}_r$. \square

Tabulated results of Section 6

6.1.1. Boxes and even star-regular mesh cells. If the mesh cell K is even (i.e., there exists $\bar{K} \in K$ such that $K \subset \bar{K} - K$), then for a regular polygon the optimal interior weight for polynomials of degree at most k is bounded above by the optimal interior weight $\bar{M}_{\circlearrowleft D}^k$ for a D -dimensional sphere. Based on equations (6.4) and (6.7), we tabulate exact values or bounding intervals for the optimal interior weight for an interval ($\bar{M}_{[0,1]}^k$), a square ($\bar{M}_{[0,1]^2}^k$), and a cube ($\bar{M}_{[0,1]^3}^k$). Note that for a tensor product polynomial space the optimal weight is $\bar{M}_{[0,1]}^k$ independent of the dimension D of the box (see Remark 6.14). Note also that for $k \leq 3$, *enforcing positivity at the cell center enforces positivity of the retentional for the optimal weight* (see Theorems 6.6 and 6.7).

k ($\mathcal{V} = \mathbb{P}_D^k$):	0, 1	2, 3	4, 5	6, 7	8, 9	10, 11
$n = \lfloor k/2 \rfloor$:	0	1	2	3	4	5
$m = \lfloor n/2 \rfloor$:	0	0	1	1	2	2
$\bar{M}_{[0,1]}^k = \frac{(n+1)(n+2)}{2}$:	1	3	6	10	15	21
$\bar{M}_{\circlearrowleft 2}^k = (m+1) \cdot \lfloor \frac{n+3}{2} \rfloor$:	1	2	4	6	9	12
$\bar{M}_{\circlearrowleft 3}^k = \frac{m+1}{3} \cdot (3 + 2\lfloor \frac{n+1}{2} \rfloor)$:	1	1.6	3.3	4.6	7	9
$\bar{M}_{[0,1]^2}^k$:	1	2	[3.5, 4]	[5.5, 6]	[8, 9]	[11, 12]
$\bar{M}_{[0,1]^3}^k$:	1	1.6	[2.6, 3.3]	[4, 4.6]	[5.6, 7]	[7.6, 9]

6.1.2. Simplices and arbitrary star-regular mesh cells. If the mesh cell is not necessarily even, then for a regular polygon the optimal interior weight is still bounded above by $\bar{M}_{\star D}^{k,+}$. Based on equations (6.5) and (6.8), as well as Remark 6.10 and Theorem 6.9, we tabulate exact values or bounding intervals for optimal interior weights for the triangle ($\bar{M}_{\Delta 2}^k$) and tetrahedron ($\bar{M}_{\Delta 3}^k$). Note that to enforce positivity of the retentional for the optimal weight, *for a quadratic representation space it is sufficient to enforce positivity at the cell center* (see Theorem 6.6), and, in the case of a simplex, *for a cubic representation space it is sufficient to also enforce positivity at the center of each face* (see Theorem 6.4). When using these weights, take the boundary average as the arithmetic average of face averages (§3.5).

k ($\mathcal{V} = \mathbb{P}_D^k$):	0	1	2	3	4	5	6	7
$n = \lfloor k/2 \rfloor$:	0	0	1	1	2	2	3	3
$\bar{M}_{[0,1]}^k = \frac{(n+1)(n+2)}{2}$:	1	1	3	3	6	6	10	10
$\bar{M}_{\star 2}^{k,+} = \frac{n+1}{2} (\lfloor \frac{k+1}{2} \rfloor + 2)$:	1	1.5	3	5	6	7.5	10	12
$\bar{M}_{\star 3}^{k,+} = \frac{n+1}{3} (\lfloor \frac{k+1}{2} \rfloor + 3)$:	1	1.25	2.6	3.3	5	6	8	9.3
$\bar{M}_{\Delta 2}^k$:	1	1	2	2.2	[3.4, 6]	[3.5, 6]	$[5 + \frac{1}{7}, 10]$	[5.25, 10]
$\bar{M}_{\Delta 3}^k$:	1	1	1.6	1.83	[2.56, 5]	[2.6, 6]	$[3 + \frac{9}{14}, 8]$	[3.75, 9.3]

Fig. 6.1: Essential results of Section 6. A bounding interval is given where the exact value is unknown.

6.3. Linear and quadratic representation spaces.

THEOREM 6.5 (linear representation space). *Let K be a star-regular polytope and let $\mathcal{V} = \mathbb{P}_D^1$. Assume that the origin is the only point whose orbit under the isometries of K is a singleton. Then the optimal interior weight is $\overline{M}^* = 1$ and the positivity-preserving time step is guaranteed simply by enforcing positivity at the boundary nodes.*

Proof. If U is a linear function then $\widehat{\mathcal{B}}(U) = 1$, as can be seen by averaging over the orbit of U under the group of isometries of the polytope. \square

THEOREM 6.6 (quadratic representation space). *Let K be a star-regular polytope, and let $\mathcal{V} = \mathbb{P}_D^2$. Assume that the origin is the only point whose orbit under the isometries of K is a singleton. Then the optimal time step is guaranteed simply by enforcing positivity at the boundary nodes and at the cell center. Enforcing positivity at the cell center is equivalent to enforcing positivity of the retentional $\overline{\mathcal{R}}^* = \overline{M}^* \overline{\mathcal{C}} - \overline{\mathcal{B}}$, where the optimal interior weight is $\overline{M}^* = \frac{D+2}{D}$.*

Proof. As seen from equation (6.1), for any homogeneous quadratic U , $\widehat{\mathcal{B}}U = \frac{D+2}{D}$. If U is a constant-valued function, then $\widehat{\mathcal{B}}U = 1$. So the optimizer cannot be constant. So by Theorem 5.10 its zero set must be nonempty. We can require the optimizer to be invariant under the isometries of the polytope. So it must be a positive rotationally invariant quadratic that has a zero at the origin, i.e. a homogeneous quadratic. The support of the optimal interior sum is therefore restricted to the origin. So the retentional is proportional to the value at the cell center. \square

6.4. Cubic representation spaces.

THEOREM 6.7 (odd-degree representation spaces for boxes). *For boxes, $\overline{M}_{[0,1]^D}^{2n+1} = \overline{M}_{[0,1]^D}^{2n}$, and likewise for other even polytopes and for spheres. In particular, for a cubic representation space, $\overline{M}^* = \frac{D+2}{D}$, and positivity of the interior sum can be enforced simply by enforcing positivity of the value at the origin.*

Proof. The isometries of an even polytope by definition include negation $\mathbf{x} \mapsto -\mathbf{x}$. Therefore an optimizer $U^* \in \mathbb{P}_D^{2k+1}$ symmetric under the isometries of the polytope lacks odd-degree terms, so $U^* \in \mathbb{P}_D^{2k}$. \square

THEOREM 6.8 (cubic representation space for simplices: optimal retentional points). *Assume that $\mathcal{V} = \mathbb{P}_D^3$. For any simplex, optimal retentional points are located at the cell center and at the centers of the faces.*

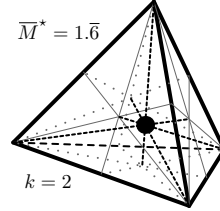
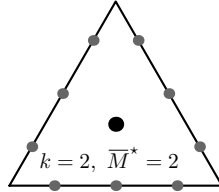
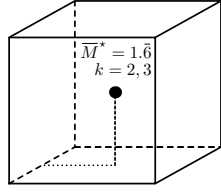
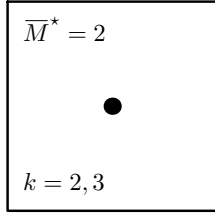
Proof. By Figure 5.1, the set of optimal retentional points must be zeros of an optimizer and can be required to be invariant under the isometries of K . Since \mathcal{V} is cubic, this means that optimal retentional points can exist only at the center of the cell and at the center of its faces. (Note that an optimizer candidate uniformly zero on the boundary could not have a boundary crowding exceeding zero.) \square

THEOREM 6.9 (cubic representation space: optimal weight for triangle and tetrahedron). *Assume that $\mathcal{V} = \mathbb{P}_D^3$. For a triangle the optimal interior weight is $\overline{M}_{\Delta_2}^3 = 20/9$, and the optimal retentional points are located at the cell center and at the centers of the edges. For a tetrahedron the optimal interior weight is $\overline{M}_{\Delta_3}^3 = 11/6$,*

REMARK 6.10. In [20], Zhang, Xia, and Shu construct a boundary-weighted quadrature rule for triangles. For representation spaces \mathbb{P}_D^{2n} and \mathbb{P}_D^{2n+1} , their rule has interior weight $\overline{M}_{[0,1]}^{2n} = \overline{M}_{[0,1]}^{2n+1} = \frac{(n+1)(n+2)}{2}$ (see equation (6.2)), showing for example that $\overline{M}_{\Delta_2}^3 \leq 3 = \overline{M}_{[0,1]}^3$.

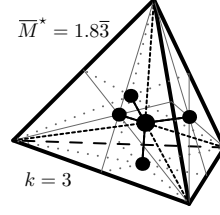
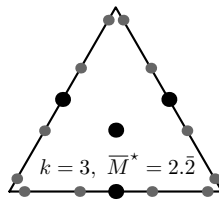
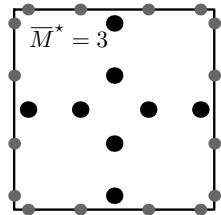
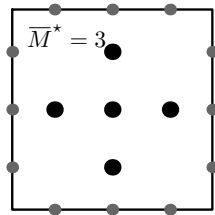
Proof (sketch). By Theorem 6.4 and Figure 5.1, we may demand an optimizer that is invariant under the isometries of K and that is zero at the center of the mesh

Key results: optimal retentional positivity points



For quadratic and cubic polynomial representation spaces, the set of optimal interior points for a box is simply the cell center (Theorems 6.6 and 6.7).

For quadratic polynomials in a simplex, the set of optimal interior points is simply the cell center (Theorem 6.6; contrast with Figure 1 in [18]).



$$\mathcal{V} = \mathbb{P}^2(x) \cdot \mathbb{P}^2(y)$$

$$\mathcal{V} = \mathbb{P}^3(x) \cdot \mathbb{P}^3(y)$$

For tensor product polynomial spaces, the optimal interior points for a box are indicated in Remark 6.14 (see [17]).

For cubic polynomials in a simplex, the set of optimal “interior” points consists of the cell center and the centers of the faces (Theorem 6.4).

Fig. 6.2: Optimal interior points for standard mesh cells and low-order polynomials. Black positivity points are retentional (i.e. “interior”) points. Gray points (when shown) are boundary nodes and depend on one’s choice of a correct boundary quadrature. The black points are determined by mesh cell geometry and the representation space and are thus independent of the choice of gray points. Enforcing positivity at the black points automatically enforces positivity of the optimal retentional $\widehat{\mathcal{R}}^* := \overline{M}^* \widehat{\mathcal{C}} - \widehat{\mathcal{B}}$ and guarantees that positivity of the cell average is maintained for the same minimum time step that one would guarantee by enforcing positivity everywhere in the mesh cell (assuming that the same wave speed caps are enforced, see Section 7.2). Positivity is also enforced at boundary nodes, but for a different purpose: to ensure that Riemann problems are solved with physical states. For a linear representation space, the set of retentional points is empty, and it is enough to enforce positivity at the boundary nodes.

cell and at the centers of its faces. Both for a triangle and for a tetrahedron, up to multiplication by a nonzero scalar there exists a unique such cubic polynomial. This polynomial is definite (i.e. positive after negating if necessary), and evaluating $\widehat{\mathcal{B}}$ for this polynomial yields the values $\frac{20}{9}$ for a triangle and $\frac{11}{6}$ for a tetrahedron. \square

Results for quadratic and cubic polynomials are summarized in Figure 6.2.

6.5. High-order representation spaces.

THEOREM 6.11 (weights for 1D interval).

$$\overline{M}_{[0,1]}^{2n} = \overline{M}_{[0,1]}^{2n+1} = \overline{W}^{-1} := \frac{(n+1)(n+2)}{2}. \quad (6.2)$$

Note that the optimal boundary-weighted quadrature is the Gauss-Lobatto quadrature with n interior points and end weight \overline{W} .

Proof. For the canonical mesh cell $K = [0, 1]$, the Gauss-Lobatto quadrature

$$2 \int_{[0,1]}^Q U = \overline{W}(U(0) + U(1)) + \sum_{i=1}^n w_i U(x_i) \quad (6.3)$$

with n interior points is exact for polynomials of degree at most $2n+1$. The function $U^*(x) = \prod_{i=1}^n (x - x_i)^2$ is zero at all interior points and is of degree $2n$. So for the representation spaces \mathbb{P}_D^{2n} and \mathbb{P}_D^{2n+1} , the quadrature rule is exact, U^* is a positive function in the representation space, and U^* is zero on the interior points. Therefore the hypotheses of Theorem 5.11 are satisfied and the conclusion follows. \square

REMARK 6.12. For 1D mesh cells, Zhang and Shu enforce positivity at the Gauss-Lobatto quadrature points, which of course implies positivity of the retentional [17].

The previous theorem is a special case of the following theorem.

THEOREM 6.13 (optimal interior weight for spherical mesh cells).

$$\overline{M}_{\mathbb{O}^D}^{2n} = \overline{M}_{\mathbb{O}^D}^{2n+1} = \frac{(\lfloor \frac{n}{2} \rfloor + 1)(2\lfloor \frac{n+1}{2} \rfloor + D)}{D}. \quad (6.4)$$

Furthermore, $\overline{M}_{[0,1]^D}^k \leq \overline{M}_{\mathbb{O}^D}^k$, with equality precisely when $D = 1$ or $k < 4$.

REMARK 6.14. For boxes one can also construct a boundary-weighted quadrature rule by taking the tensor product of a Gauss-Lobatto quadrature rule with a quadrature rule used to integrate over a face and averaging over all D such quadrature rules, as is done in [17] for the case $D = 2$. The resulting interior weight is $\overline{M}^* = \overline{M}_{[0,1]}^k$ independent of D . This weight and set of quadrature points is optimal for a tensor product polynomial space; indeed, invoking Corollary 5.11, a confirming optimizer is $U^*(\mathbf{x}) := \prod_{i=1}^D U_{[0,1]}^{k,*}(x_i)$, where $U_{[0,1]}^{k,*}$ is a unit-interval optimizer. But for \mathbb{P}_D^k , in case $D > 1$ and $k > 1$, the boundary weight of this theorem is an improvement over $\overline{M}_{[0,1]}^k$.

Proof (sketch). Recall from (6.1) that $\overline{\mathcal{C}} = D \int_0^1 r^{D-1} \overline{\mathcal{B}}_r dr$, and observe that, for boxes and spheres, $\overline{\mathcal{B}}_r$ is an even polynomial in r of degree less than or equal to the degree k of the representation space. So we can write $\overline{\mathcal{B}}_r = B(r^2)$, where $\deg B = \lfloor k/2 \rfloor$. We seek a quadrature rule that maximizes the weight on the point $r = 1$. Making the substitution $t = 1 - 2r^2$ shows that $\overline{\mathcal{C}}$ is given by an integral with a Jacobi weight function.

In case $k = 4m$ (or $k = 4m + 1$) we use a Gauss-Radau quadrature rule for Jacobi weight (GRJ) with m interior points, which is exact for polynomials of degree at most $2m$ (see [3]). In the case of a spherical mesh cell, an optimizer that confirms that the boundary weight is maximal is $U^*(r^2) = \prod_{i=1}^m (r^2 - r_i^2)^2$, where the r_i are the interior quadrature points corresponding to the interior quadrature points t_i of the GRJ quadrature rule.

In case $k = 4m + 2$ (or $k = 4m + 3$), we use a Gauss-Lobatto quadrature rule for Jacobi weight (GLJ) with m interior points, which is exact for polynomials of degree at most $2m+1$ (see [4]). In the case of a spherical mesh cell, an optimizer that confirms

that the boundary weight is maximal is $U^*(r^2) = r^2 \prod_{i=1}^m (r^2 - r_i^2)^2$, where the r_i are the interior quadrature points corresponding to the interior quadrature points t_i of the GLJ quadrature rule. \square

THEOREM 6.15 (admissible interior weight for any star-regular mesh cell).

$$\overline{M}_{\Delta^D}^k \leq \overline{M}_{\star^D}^{k,+} := \frac{(\lfloor \frac{k}{2} \rfloor + 1)(\lfloor \frac{k+1}{2} \rfloor + D)}{D}. \quad (6.5)$$

REMARK 6.16. Equality holds only for the case $\overline{M}_{\Delta^D}^0 = 1$. Recall from Remark 6.10 that $\overline{M}_{\Delta^2}^{2n} \leq \overline{M}_{\Delta^2}^{2n+1} \leq \frac{(n+1)(n+2)}{2}$, which agrees with estimate (6.5) for even-dimensional representation spaces and for odd-dimensional representation spaces is slightly better than estimate (6.5).

Proof (sketch). We want a quadrature rule with such weight on the boundary average for $\overline{\mathcal{C}} = D \int_0^1 r^{D-1} \overline{\mathcal{B}}_r dr$. Unlike for boxes and spheres, we cannot assume that $\overline{\mathcal{B}}_r$ is an even polynomial. For \mathbb{P}_D^{2n} we use a GRJ quadrature (see [3]) with n points to get a quadrature rule for $\overline{\mathcal{C}}$, and for \mathbb{P}_D^{2n+1} we use a GLJ quadrature (see [4]) with n points to get a quadrature rule for $\overline{\mathcal{C}}$; in each case, the resulting end weight is the reciprocal of the interior weight appearing in (6.5). \square

6.6. Lower bounds for interior weights. In the previous sections we computed exact values and upper bounds for optimal interior weights. In the case of higher-order representation spaces where we have merely computed upper bounds, we would also like to have a lower bound that suggests how much the estimate might be improved. In particular, we will obtain bounding intervals that prove that

$$\overline{M}_{\circ^D}^k = \Omega(k^2), \quad \overline{M}_{[0,1]^D}^k = \Omega(k^2), \quad \text{and} \quad \overline{M}_{\Delta^D}^k = \Omega(k^2). \quad (6.6)$$

Recall that for 1D intervals the optimal weight is given by equation (6.2). For boxes and for simplices, we now bootstrap from this result to obtain lower bounds for the interior weight.

6.6.1. Boxes. First consider the case of the box $[0, 1]^D$. It has $2D$ faces, each of which is a box of dimension $D - 1$. Each face has $2(D - 1)$ sub-faces, each of which is a box of dimension $D - 2$. Suppose that U is defined on the $x = 1$ face of the box and has interior weight $\overline{M}_{[0,1]^{D-1}}^{k,-}$ when restricted to this face. Then U can also be thought of as a function on $[0, 1]^D$ and has boundary weight given by the recurrence relation

$$\overline{M}_{[0,1]^D}^{k,-} = \frac{1 + (D - 1)\overline{M}_{[0,1]^{D-1}}^{k,-}}{D}, \quad (6.7)$$

as will be shown in detail in Part II of this work [7]; we can take $\overline{M}_{[0,1]}^{k,-} := \overline{M}_{[0,1]}^k$. By induction on D , the recurrence relation (6.7) implies that $\overline{M}_{[0,1]^D}^k = \mathcal{O}(k^2)$, so by Theorem 6.13, $\overline{M}_{[0,1]^D}^k = \Omega(k^2)$.

6.6.2. Simplices. Let K be a regular simplex of dimension D . Suppose that U is a polynomial of degree at most k defined on the face F of K not containing vertex V , and suppose that U is positive when restricted to F . Then U extends uniquely to

Prescriptions for positivity limiting

Check positivity efficiently. One can use interval arithmetic to inexpensively confirm cell positivity in the vast majority of mesh cells. For nodal DG, choose positivity points to be nodal points to avoid additional computational expense. See §7.1.

Pad inequalities. In practice, error in machine arithmetic makes it problematic to enforce exact inequalities such as $\rho \geq 0$ or $p \geq 0$. Instead, enforce $\rho \geq \epsilon_\rho$ or $p \geq \epsilon_p$ for some small $\epsilon_\rho > 0$ and $\epsilon_p > 0$. See [14].

Use positivity points to improve stability. Enforcing positivity at additional interior points may improve stability (likely depending on the choice of oscillation-suppressing limiters). Since values used in volume and boundary quadratures must be calculated (or available) anyway, positivity of these values can be efficiently enforced, and enforcing positivity at the points guarantees that state values used in the numerical method are always positive. For modal DG, positivity at any finite set of points can be efficiently checked, and it makes sense to include the optimal retentional points if they are known.

Use wave speed desingularization for systems, especially for shallow water. When enforcing positivity in shallow water, fluxes need to be calculated with remapped states in order to desingularize wave speeds. See remarks in Algorithm 1 and Algorithm 2 and Section 7.2. For gas dynamics, wave speed desingularization is needed when enforcing positivity of the density (although more often it is positivity of the pressure that needs to be enforced).

Estimate an optimal time step after enforcing the cell positivity condition. The factor by which the time step must be shortened determines the expense of positivity limiting (§7.3). Enforcing the cell positivity condition guarantees a minimum time step Δt_{pos} that preserves positivity of the cell average; see equation (3.4). One can directly calculate the maximum one-stage time step Δt_{zero} that maintains positivity of the cell average (§4.1) in addition to calculating the maximum stable time step Δt_{stable} to determine an optimal safe time step. For multistage and local time stepping, one can use Δt_{stable} , Δt_{zero} , and optionally Δt_{pos} to maintain and iteratively adjust an estimate of a safe time step that is both stable and positivity-preserving.

Fig. 7.1: Key points of Section 7.

a polynomial that is homogeneous of degree k when expanded about V . This yields a recurrence relation for a lower bound $\bar{M}_{\Delta^D}^{k,-} \leq \bar{M}_{\Delta^D}^k$,

$$\bar{M}_{\Delta^D}^{k,-} = \left(\frac{D+k}{D} \right) \left(\frac{1 + D \frac{D-1}{D+k-1} \bar{M}_{\Delta^{D-1}}^{k,-}}{1+D} \right), \quad (6.8)$$

as will be shown in detail in Part II of this work [7]. By induction on D , recurrence relation (6.8) implies that $\bar{M}_{\Delta^D}^k = \mathcal{O}(k^2)$. Thus, by Theorem 6.15, $\bar{M}_{\Delta^D}^k = \Omega(k^2)$.

7. Practical application of positivity limiting. We briefly consider the most prominent issues that arise when enforcing positivity. Detailed treatment of practical issues is deferred to Part II of this work [7]. We summarize in Figure 7.1.

7.1. Efficient implementation of positivity checks. For almost all problems, in the large majority of cells one can confirm that the solution is positive and will remain so for any stable time step by using interval arithmetic. Thus, one can enforce positivity with little additional computational expense per time step. For example, in the case of gas dynamics, one can quickly confirm positivity of the pressure in the vast majority of cells by checking that $P_{\min} := \rho_{\min} \mathcal{E}_{\min} - \mathbf{m}_{\max}^2/2$ is positive, where ρ_{\min} and \mathcal{E}_{\min} are lower bounds on density and energy in the cell and \mathbf{m}_{\max} is an upper bound on momentum.

The question is how to obtain a tuple of intervals $[\underline{u}_{\min}, \underline{u}_{\max}]$ for the components of the conserved variables. In modal DG one can obtain lower and upper bounds that hold globally in the mesh cell by using lower and upper bounds on the polynomial basis functions φ_j . This works well, because for smooth solutions the coefficients of higher-order modes decay rapidly as the mesh is refined. Nodal DG represents the solution using values at nodes; therefore, one can easily obtain an interval $[\underline{u}_{\min}, \underline{u}_{\max}]$ that applies to all nodal values. Thus, even for nodal DG, checking positivity at all nodes is usually no more expensive than checking positivity at a point. By Theorem 5.3, positivity at the nodes of a nodal DG scheme implies positivity of a retentional with weight $\overline{W} \leq \overline{W}^*$, because the cell average is a positively weighted sum of values at the nodes (including boundary nodes) and so is a boundary-weighted quadrature.

7.2. Wave speed desingularization is needed when limiting density. Let ρ denote depth in the shallow water case or density in the gas dynamics case. After enforcing positivity of ρ at boundary nodes, wave speeds need to be de-singularized. This can be done by modifying states used to compute fluxes when the wave speed exceeds an estimate of the maximum wave speed in the physical solution.

In both shallow water and gas dynamics, desingularization of momentum (i.e. fluid velocity) is necessary. Let u_{cap} be a fluid speed cap that, for a sufficiently refined mesh, is guaranteed to exceed the fluid speed that arises in the exact solution. Then an accuracy-respecting desingularization map of the momentum (or fluid velocity) is the rescaling $\mathbf{u} \leftarrow \mathbf{u} \cdot R_1(u_{\text{cap}}/|\mathbf{u}|)$, where $R_1(x) = 1$ if $x \geq 1$ and equals x (or the spline $x(2-x)$) if $0 \leq x \leq 1$ (see Section 4.4 of [1]).

For shallow water, enforcing positivity means enforcing positivity of ρ and therefore essentially always entails wave speed desingularization. For gas dynamics, in addition to desingularizing the fluid speed \mathbf{u} , it may also be necessary to desingularize the sound speed $c = \sqrt{\gamma\theta}$, e.g. by capping the pseudo-temperature $\theta := p/\rho$.

More careful study of wave speed desingularization is left to future work.

7.3. Cost of positivity limiting. For most problems, for the vast majority of cell updates, a quick check (§7.1) will confirm that positivity limiting is unnecessary. If local time stepping is used, then the total cost of positivity limiting will be marginal. But if global time stepping is used, then the expense of positivity limiting is measured by the factor by which the time step must be shortened to maintain positivity. This suggests (1) a careful consideration of how to obtain tight and reliable wave speed bounds for use in wave speed desingularization and (2) a comparison of stable and positivity-preserving time steps.

For (2), in the case of one-dimensional mesh cells with k th order polynomial space, values are known: an approximate value for the maximum stable time step is given by $\Delta t_{\text{stable}}^{-1} \approx (k+1/2)\lambda/\Delta x$ if an SSP-RK time-stepping method of order k is used (see Table 2.2 in [2]); in comparison, capping boundary crowding by $\overline{M}^* = (n+1)(n+2)/2$ gives $\Delta t_{\text{pos}}^{-1} = \lambda \overline{M}^* = (n+1)(n+2)\lambda/\Delta x$, where k equals $2n$ or $2n+1$.

7.4. Isoparametric mesh cells. For a typical isoparametric mesh cell, in canonical coordinates the mesh cell is a box or simplex and the representation space is a polynomial space (e.g. \mathbb{P}_D^k). Each physical mesh cell is the image of such a canonical mesh cell under a diffeomorphism ϕ , and the physical representation space is the push-forward under ϕ of the canonical representation space. The outflow positivity limiting framework is defined in canonical coordinates and can be applied without modification for isoparametric mesh cells: under reasonable regularity assumptions on ϕ , direct application of positivity limiters in canonical coordinates respects accuracy and guarantees a minimum positivity-preserving time step [7].

8. Conclusion. This work consists of two main results: a framework and algorithm for positivity limiting, and calculations of optimal weights and positivity points needed by this framework.

8.1. Outflow positivity limiting framework. We have developed a framework for preserving positivity of each cell average based on limiting the rate and amount of material that can flow out of the cell. This is achieved by linear damping of high-order corrections, remapping boundary node states to limit wave speeds, and limiting the time step. In each cell, the high-order corrections are linearly damped just enough to enforce a physically justified cap $\bar{M} > 1$ on the *boundary crowding* $\widehat{\mathcal{B}}A(U) := \frac{\bar{\mathcal{B}}A(U)}{\bar{\mathcal{C}}A(U)}$ for all affine functionals A in a set of state positivity functionals \mathcal{P}^* , where $\bar{\mathcal{C}}$ is the cell average and $\bar{\mathcal{B}}$ is the arithmetic average over all faces of the average over each face (see Section 3.8); this condition is satisfied precisely when the *unital retentional*

$$\widehat{\mathcal{R}}(U) = \frac{\bar{M}\bar{\mathcal{C}}U - \bar{\mathcal{B}}U}{\bar{M} - 1}$$

satisfies positivity. One way to enforce positivity of the unital retentional is to enforce that the solution is positive at appropriately chosen quadrature points in the mesh cell, as Zhang and Shu have done [16, 18]. Directly enforcing positivity of the unital retentional is computationally inexpensive and makes it unnecessary to determine and enforce positivity at these points. For concreteness, we display positivity-preserving algorithms for scalar conservation laws and shallow water (Algorithm 1) and for gas dynamics (Algorithm 2).

8.2. Optimal weights and positivity points. Just as point-wise positivity limiting prompts the search for optimal positivity points, retentional positivity limiting prompts the need for a reasonably close upper bound \bar{M} on the optimal interior weight $\bar{M}_K^*(\mathcal{V})$. In Section 5, we developed a general framework to estimate upper and lower bounds on $\bar{M}_K^*(\mathcal{V})$. In Section 6, we applied this framework to tabulate interior weights for boxes and simplices for polynomial representation spaces.

In practice, the canonical mesh cell is almost always a cube or a simplex, and, for problems that are likely to entail positivity limiting, the representation space is likely to be a space of polynomials of at most cubic degree. Assuming these conditions, the set of optimal interior positivity points is very small, and the essential take-home result of this work is that to guarantee the same positivity-preserving time step as if positivity were enforced everywhere in the mesh cell, in addition to enforcing positivity (and, for shallow water, desingularizing wave speeds) at boundary nodes, *it is sufficient to enforce positivity at the cell center*, except that for a simplex with a cubic representation space one must also enforce positivity at the centers of the faces. See Figure 6.2.

$\mathcal{P} \subset \mathbb{R}^N$	set of positive states	$X \subset \mathbb{R}^D$	set of positivity points
$\mathcal{P}^* \subset \{A : \mathbb{R}^N \rightarrow \mathbb{R}\}$	affine posit. functionals	$\lambda/2 > 0$	speed cap on Q
$K \subset \mathbb{R}^D$	canonical mesh cell	$\bar{\lambda} := \frac{\lambda}{V}$	scale-invariant version
$\mathbb{P}_D \subset \{f : \mathbb{R}^D \rightarrow \mathbb{R}\}$	polynomials in D vars.	$h \leq \lambda U^-$	numerical flux
$\mathbb{P}_D^k \subset \mathbb{P}_D$	polynomials of deg. $\leq k$	$\bar{h} := \frac{h}{V}$	scale-invariant version
$\mathcal{V} \ni \mathbb{P}_D^k$	representation space	$\bar{U}^{n+1} := \bar{C}U - \Delta t \bar{B}\bar{h}$	updated cell average
$V := K := \int_K 1$	measure of cell	$\bar{W} \geq \Delta t \bar{\lambda}$	boundary weight
$A := \partial K := \oint_{\partial K}^Q 1$	measure of boundary	$\bar{\mathcal{R}}_{\bar{W}} := \bar{C} - \bar{W}\bar{B}$	retentional
$\mathcal{C}(U) := \int_K U$	cell integral	$\bar{\mathcal{R}}^{\bar{M}} := \bar{M}\bar{C} - \bar{B}$	retentional (rescaled)
$\bar{\mathcal{C}}(U) := \bar{U} := \frac{1}{V} \int_K U$	cell average	$\widehat{\bar{B}}(U) := \bar{B}(U)/\bar{C}(U)$	boundary crowding
$Q = \partial^Q K \subset \partial K$	boundary quadrature pts.	$\mathcal{V}_K^+ \subset \mathcal{V} \setminus \{0\}$	functions positive in K
$\mathcal{B}(U) := \oint_{\partial K}^Q U^-$	boundary integral quad.	$\bar{M}_K^* := \sup \widehat{\bar{B}}(\mathcal{V}_K^+)$	optimal interior weight
$\bar{\mathcal{B}}(U) := A^{-1} \oint_{\partial K}^Q U^-$	boundary avg. quad.	$\bar{M} := \bar{W}^{-1} \geq \bar{M}_K^*$	admissible weight

Fig. 8.1: Key definitions for cell positivity.

Acknowledgements. This work was supported in part by NSF grant DMS-1016202.

REFERENCES

- [1] A. Bollermann, S. Noelle, and M. Lukáčová-Medvid'ová, *Finite volume evolution Galerkin methods for the shallow water equations with dry beds*, Communications in Computational Physics **10** (2011), 371–404.
- [2] B. Cockburn and C.-W. Shu, *Runge-Kutta discontinuous Galerkin methods for convection-dominated problems*, J. Sci. Comput. **16** (2001), no. 3, 173–261.
- [3] W. Gautschi, *Gauss–Radau formulae for Jacobi and Laguerre weight functions*, Mathematics and Computers in Simulation **54** (2000), 403–412.
- [4] ———, *High-order Gauss-Lobatto formulae*, Numerical Algorithms **25** (2000), 213–222.
- [5] S. K. Godunov, *A difference method for numerical calculation of discontinuous solutions of the equations of hydrodynamics*, Mat. Sb. (N.S.) **47(89)** (1959), no. 3, 271–306.
- [6] A. Harten, P.D. Lax, and B. van Leer, *On upstream differencing and Godunov-type schemes for hyperbolic conservation laws*, SIAM Review **25** (1983), 35–61.
- [7] E.A. Johnson, *Outflow positivity limiting for hyperbolic conservation laws. Part II: Analysis and extension*, manuscript in preparation.
- [8] R.J. LeVeque, *Finite volume methods for hyperbolic problems*, Cambridge University Press, 2002.
- [9] T.-P. Liu and J. A. Smoller, *On the vacuum state for the isentropic gas dynamics equations*, Advances in Applied Mathematics **1** (1980), 345–359.
- [10] X.-D. Liu and S. Osher, *Nonoscillatory high order accurate self-similar maximum principle satisfying shock capturing schemes*, SIAM J. Numer. Anal. **33** (1996), no. 2, 760–779.
- [11] B. Perthame and C.-W. Shu, *On positivity preserving finite volume schemes for Euler equations*, Numer. Math. **73** (1996), 118–130.
- [12] W. Rudin, *Functional analysis*, second ed., McGraw-Hill, 1991.
- [13] V.V. Rusanov, *Calculation of interaction of non-steady shock waves with obstacles*, J. Comp. Math. Phys. USSR **1** (1961), 267–279.
- [14] C. Wang, X. Zhang, C.-W. Shu, and J. Ning, *Robust high order discontinuous Galerkin schemes for two-dimensional gaseous detonations*, J. Comp. Phys. (2011), 653–665.
- [15] X. Zhang, *Maximum-principle-satisfying and positivity-preserving high order schemes for conservation laws*, Ph.D. thesis, Brown University, Providence, Rhode Island, May 2011.
- [16] X. Zhang and C.-W. Shu, *On maximum-principle-satisfying high order schemes for scalar conservation laws*, J. Comp. Phys. **229** (2010), 3091–3120.
- [17] ———, *On positivity preserving high order discontinuous Galerkin schemes for compressible*

- Euler equations on rectangular meshes*, J. Comp. Phys. **229** (2010), 8918–8934.
- [18] ———, *Maximum-principle-satisfying and positivity-preserving high-order schemes for conservation laws: Survey and new developments*, Proc. R. Soc. A **467** (2011), 2752–2776.
- [19] ———, *Positivity-preserving high order discontinuous Galerkin schemes for compressible Euler equations with source terms*, J. Comp. Phys. **230** (2011), 1238–1248.
- [20] X. Zhang, Y. Xia, and C.-W. Shu, *Maximum-principle-satisfying and positivity-preserving high order discontinuous Galerkin schemes for conservation laws on triangular meshes*, J. Sci. Comput. **50** (2012), no. 1, 29–62.

Algorithm 1 Positivity-preserving Euler time-step for scalar conservation laws and shallow water.

For shallow water, U , h , and \mathbf{f} represent the first component of \underline{U} , \underline{h} , and $\underline{\mathbf{f}}$, respectively. For the canonical mesh cell K and representation space \mathcal{V} determine an admissible weight \bar{M} such that $\bar{\mathcal{R}}^{\bar{M}}U := \bar{M}\bar{U} - \bar{\mathcal{B}}U > 0 \ \forall U = \sum_i U^i \varphi_i > 0$ (see Figure 6.1), where $\bar{\mathcal{B}}U = \sum_j U^j \bar{\mathcal{B}}(\varphi_j)$ is the boundary average (see §3.5). For efficiency, precompute the values $\bar{\mathcal{B}}(\varphi_j)$.

1. $\forall K$ rescale the deviation $d\underline{U}$ from the cell average \bar{U} by a percentage θ_Y , damping just enough so that $U > 0$ at a set of positivity points X that includes all quadrature points in $\oint_{\partial K}^Q$ and so that $\bar{\mathcal{R}}^{\bar{M}}(U) = \bar{M}\bar{U} - \bar{\mathcal{B}}U > 0$:

$$\begin{aligned} \underline{U} &:= \underline{U}^n, \quad \bar{U} := \bar{C}\underline{U}, \quad d\underline{U} := \underline{U} - \bar{U}, \quad U_{\min} = \min_{\mathbf{x} \in X} U, \\ \theta_X &= \min \left\{ 1, \frac{\bar{U}}{\bar{U} - U_{\min}} \right\}, \quad \theta_{\bar{\mathcal{R}}^{\bar{M}}} = \min \left\{ 1, \frac{(\bar{M} - 1)\bar{U}}{\bar{\mathcal{B}}(d\underline{U})} \right\}, \quad \theta_Y := \min(\theta_X, \theta_{\bar{\mathcal{R}}^{\bar{M}}}), \\ \underline{U} &\leftarrow \bar{U} + \theta_Y d\underline{U}. \end{aligned}$$

If X is sufficiently rich (see Figure 5.1) then $\theta_X \leq \theta_{\bar{\mathcal{R}}^{\bar{M}}}$ and computing $\theta_{\bar{\mathcal{R}}^{\bar{M}}}$ is unnecessary.

2. Compute a safe time-step Δt :

$$(\Delta t_{\text{zero}})^{-1} = \max_{\text{all } K} \left(\frac{\oint_{\partial K}^Q h(U^-, U^+, \hat{\mathbf{n}})}{\int_K U} \right), \quad \Delta t^{-1} = \max \left\{ (\alpha_z \Delta t_{\text{zero}})^{-1}, (\Delta t_{\text{stable}})^{-1} \right\},$$

where Δt_{stable} is the maximum stable time-step and $0 < \alpha_z < 1$ is a safety factor.

3. (for shallow water, not scalar case.) Modify the boundary node states \underline{U}_Q^- if necessary in order to desingularize wave speeds at boundary nodes (see §7.2).

4. $\forall K$ update the solution:

$$\int_K \underline{U}^{n+1} \varphi^j = \int_K \underline{U} \varphi^j + \Delta t \int_K \underline{\mathbf{f}}(t^n, \mathbf{x}, \underline{U}) \cdot \nabla \varphi^j - \Delta t \oint_{\partial K}^Q \underline{h}(\underline{U}_Q^-, \underline{U}_Q^+, \hat{\mathbf{n}}) \varphi^j.$$

Algorithm 2 Positivity-preserving Euler time-step for gas dynamics (cf. §3.2 of [16]).

Choose large enough values $\epsilon_\rho > 0$ and $\epsilon_p > 0$ that vanish with machine epsilon.

1. $\forall K$ evaluate the solution $\underline{U}^n =: \underline{U} = \bar{\underline{U}} + d\underline{U}$ at a set of positivity points X which includes the set of boundary nodes Q (i.e. the quadrature points of $\mathcal{f}_{\partial K}^Q$) to determine the nodal states $\underline{U}_X \supset \underline{U}_Q^-$.

2. $\forall K$ linearly damp the high-order corrections $d\underline{U}$ by a percentage θ_ρ , damping just enough so that the density ρ is positive at the points X and so that the density retentional $\bar{\mathcal{R}}^{\bar{M}}(\rho) = \bar{M}\bar{\rho} - \bar{\mathcal{B}}\rho$ is positive:

$$\begin{aligned} \theta_X &= \min \left\{ 1, \frac{\bar{\rho} - \epsilon_\rho}{\bar{\rho} - \rho_{\min}} \right\}, & \rho_{\min} &= \min_{\mathbf{x} \in X} \rho, \\ \theta_{\bar{\mathcal{R}}^{\bar{M}}} &= \begin{cases} 1 & \text{if } \bar{\mathcal{B}}(d\rho) \leq (\bar{M} - 1)\bar{\rho} - \epsilon_\rho, \\ \frac{(\bar{M} - 1)\bar{\rho} - \epsilon_\rho}{\bar{\mathcal{B}}d\rho} & \text{if } \bar{\mathcal{B}}(d\rho) > (\bar{M} - 1)\bar{\rho} - \epsilon_\rho, \end{cases} \\ \underline{U} &\leftarrow \bar{\underline{U}} + \theta_\rho d\underline{U}, & \underline{U}_X &\leftarrow \bar{\underline{U}} + \theta_\rho d\underline{U}_X, & \theta_\rho &:= \min(\theta_X, \theta_{\bar{\mathcal{R}}^{\bar{M}}}). \end{aligned}$$

3. $\forall K$ linearly damp the solution just enough so that the pressure is positive at the points X :

$$\begin{aligned} \theta_p &:= \max \left\{ \theta \in [0, 1] : (\forall \mathbf{x} \in X) p(\bar{\underline{U}} + \theta d\underline{U}(\mathbf{x})) \geq \epsilon_p \right\}, \\ \underline{U} &\leftarrow \bar{\underline{U}} + \theta_p d\underline{U}, & \underline{U}_Q^- &\leftarrow \bar{\underline{U}} + \theta_p d\underline{U}_Q^-. \end{aligned}$$

4. Modify the boundary node states \underline{U}_Q^- if necessary in order to desingularize wave speeds at boundary nodes (see §7.2).

5. $\forall K$ and for some admissible interior weight \bar{M} linearly damp $d\underline{U}$ so that the retentional $\bar{\mathcal{R}}^{\bar{M}}\underline{U} := \bar{M}\bar{\underline{U}} - \mathcal{f}_{\partial K}^Q \underline{U}_Q^-$ is positive:

$$\begin{aligned} \theta_Q &:= \max \left\{ \theta \in [0, 1] : p((\bar{M} - 1)\bar{\underline{U}} - \theta \bar{\mathcal{B}}d\underline{U}_Q^-) \geq 0 \right\}, \\ \underline{U} &\leftarrow \bar{\underline{U}} + \theta_Q d\underline{U}, & \underline{U}_Q^- &\leftarrow \bar{\underline{U}} + \theta_Q d\underline{U}_Q^-. \end{aligned}$$

6. Compute a stable, positivity-preserving time-step Δt :

$$\Delta t := \alpha_z \max_{\text{all } K} \left\{ \Delta t \in [0, \alpha_z^{-1} \Delta t_{\text{stable}}] : p \left(\int_K \underline{U} - \Delta t \mathcal{f}_{\partial K}^Q \underline{h}(\underline{U}_Q^-, \underline{U}_Q^+) \right) \geq 0 \right\},$$

where Δt_{stable} is the maximum stable time-step and $0 < \alpha_z < 1$ is a safety factor.

7. $\forall K$ update the solution:

$$\int_K \underline{U}^{n+1} \varphi^j = \int_K \underline{U} \varphi^j + \Delta t \int_K^Q \mathbf{f}(t^n, \mathbf{x}, \underline{U}) \cdot \nabla \varphi^j - \Delta t \mathcal{f}_{\partial K}^Q \underline{h}(\underline{U}_Q^-, \underline{U}_Q^+, \hat{\mathbf{n}}) \varphi^j.$$
